Hubble Space Telescope

Wide Field Camera 3

Capabilities and Scientific Programs

WFC3 Scientific Oversight Committee
and
WFC3 Science Integrated Product Team

Edited by M. Stiavelli and R. W. O'Connell

Index

1. Executive Summary

The Wide Field Camera 3 (WFC3) will be installed on the *Hubble Space Telescope* (HST) during Servicing Mission 4 in 2003. It is designed to ensure that the superb imaging performance of HST is maintained through the end of the mission. WFC3 takes advantage of recent developments in detector technology to provide new and unique capabilities for HST. Its ultraviolet/optical and near-infrared channels offer high sensitivity and wide field of view over the broadest wavelength range of any HST instrument. In the near-ultraviolet, its combination of field size and sensitivity outperforms earlier instruments by a factor of eight. In the near-infrared, it will be a factor of fifteen more capable than the earlier HST NICMOS instrument, and it offers a potent combination of resolution, field size, wavelength coverage, sensitivity, and photometric precision, which cannot easily be matched by even the largest ground-based telescopes.

WFC3's panchromatic performance allows it to address a number of major problems within NASA's Origins theme better than any previous instrument on HST. These include establishing the star-formation history of nearby galaxies, following the assembly of galaxies during the period of peak star formation and metal production activity 8-12 billion years ago, searching for the "End of the Dark Ages" - the high-redshift transition between the neutral and ionized epochs of the universe, exploring the birth and death of stars, and studying water and ices on Mars and the satellites of the outer planets. WFC3, with its superior sensitivity, spatial resolution, and wavelength coverage, will be a key instrument in exploiting the rich territory revealed by upcoming NASA ultraviolet and near-infrared missions, and by large ground-based visible and infrared surveys.

The design of WFC3 has been reviewed and endorsed by over 80 senior members of the astronomical community on seven different advisory panels. An Integrated Product Team representing a partnership between NASA Goddard Space Flight Center, the Space Telescope Science Institute, the Jet Propulsion Laboratory, and industry, is responsible for the design, fabrication, and testing of WFC3. A Scientific Oversight Committee of 21 members provides scientific guidance.

2. Introduction

A primary legacy of the *Hubble Space Telescope* (HST), both scientifically and in the public eye, will be the spectacular images it produces of the astronomical sky. Its cameras have been among the most productive instruments in the history of astronomy. As HST begins a second decade of operations, its superb imaging performance must continue to be maintained. Accordingly, a new high-performance, panchromatic camera, the *Wide Field Camera 3* (hereafter WFC3), is being developed for installation on HST during Servicing Mission 4, planned for 2003.

Three main drivers have inspired the current design of WFC3: (1) WFC3 must be able to offer excellent visible-band imaging performance which will endure until the end of the HST mission; (2) in order to address a wide variety of astrophysical questions and greatly expand HST's imaging capabilities, WFC3 should provide high sensitivity and large field of view (FOV) in the near-UV and near-IR bands; (3) as a pathfinder for NGST, WFC3 will help refine the questions that NGST will answer by providing complementary UV data and the highest near-IR sensitivity available before NGST. Although it builds on components and designs from the original WF/PC, ACS, and NICMOS, WFC3 has been able to take advantage of recent developments in both UV-visible and near-infrared detector technology to provide it with high sensitivity from 2000 to 17000 Å. This ***panchromatic*** capability makes WFC3 a unique instrument in addressing questions in three of NASA's Origins themes: The Distant Universe; Galaxies and the Nearby Universe; and Stars and Planets.

WFC3 will be the only HST scientific instrument to have been developed as a "facility instrument." That is, it was not proposed by a Principal Investigator and will not be built by an Investigation Definition Team (IDT) to answer a specific set of scientific questions. In place of an Instrument IDT, WFC3 is being designed and built by an Integrated Product Team (IPT) that includes personnel from the NASA Goddard Space Flight Center, the Space Telescope Science Institute, the Jet Propulsion Laboratory, and industry. A Scientific Oversight Committee (SOC) of 21 members was selected on the basis of community solicitation to advise the HST Senior Scientist at the NASA Goddard Space Flight Center (GSFC) and the STScI Director, and to provide broad scientific direction and guidance to the WFC3 project.

WFC3 is the product of a community consensus that HST's imaging capabilities needed to be safeguarded and enhanced in the second decade of HST life. Reviews by advisory committees, including over 80 astronomers, reflect this consensus. In 1996, the *HST and Beyond* study, chaired by A. Dressler, recommended that HST should continue to be operated as an "essential astronomical tool throughout the first decade of the next century." In 1998, the HST Project re-convened the original Instrument Peer Review panel that reviewed instrument proposals for Servicing Mission 4, to discuss the best way to ensure continued imaging capability until the HST end of mission. The panel strongly endorsed the plan to build WFC3 and install it in the telescope during Servicing Mission 4. The initial plan was for a CCD camera to operate in the visible/ultraviolet 2000 - 10000 Å spectral region. The *HST Second Decade* study panel, chaired by R. Brown, recommended that the WFC3 project consider taking advantage of the rapid improvement in IR detector technology by adding an infrared channel to cover the 9000-17000 Å spectral region. This proposal received the strong endorsement of the WFC3 Scientific Oversight

Committee, the Cycle 8 HST Time Allocation Committee, the Space Telescope Institute Council, the Space Telescope Users Committee, and the Origins Sub-Committee.

This document is a joint effort by the SOC and the WFC3 IPT to present the scientific rationale for the capabilities of WFC3. In particular, it defines the role of WFC3 as a scientific instrument aboard HST, delineates the major astronomical regimes it will explore, and shows how these have led to the final instrument design and characteristics.

3. WFC3 Science Overview

3.1 Instrument Description and Unique Scientific Capabilities

WFC3 will both physically and functionally replace the current Wide Field and Planetary Camera 2 (WFPC2) in the radial instrument bay of HST. WFPC2 is a wide-field, UV-visible imaging camera. Installed in HST in 1993, WFPC2 covers the wavelength range 1200-10500 Å. The initial motivation for WFC3 was to provide backup imaging capability for HST in the period beginning with the fourth servicing mission until the HST end of the mission (i.e. nominally the period 2003-2010). However, the initial instrument concept evolved into the present design of WFC3, which, beyond its backup role, offers new scientific capabilities in both the near-ultraviolet and near-infrared spectral domains (see Figure 1.) WFC3 takes advantage of improvements in detector technology, special optical coatings, thermo-electric cooling techniques, and filter selection to achieve new and unique science capabilities.

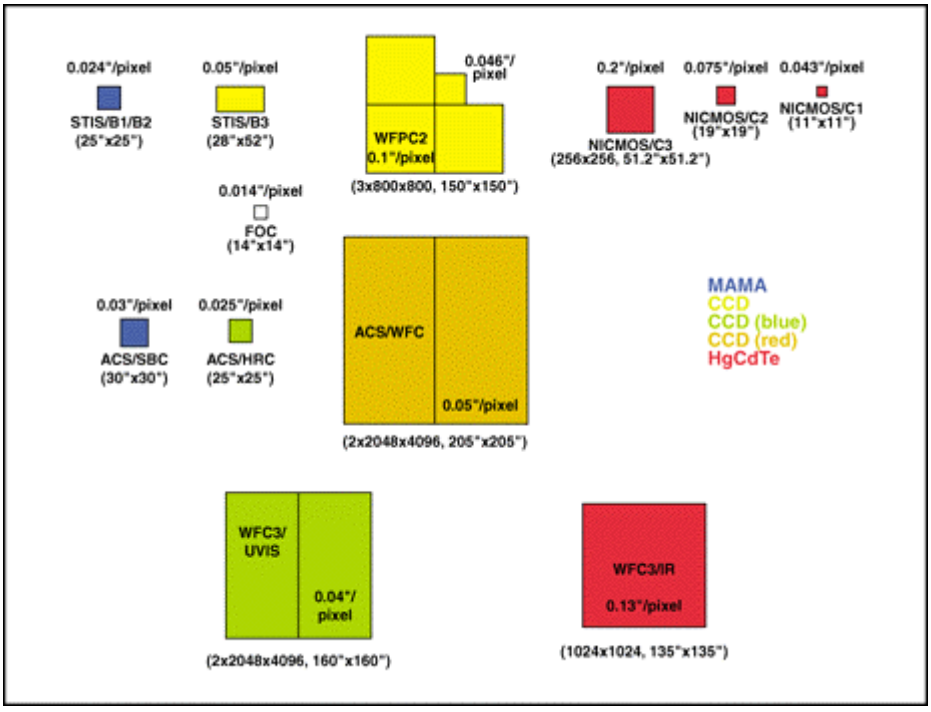

Figure 1. Comparison of the field of view of HST imaging instruments. WFC3 offers a UV-visible field of view comparable to that of ACS/WFC and WFPC2, but with enhanced UV sensitivity, and a near-infrared field of view seven times larger than NICMOS/Camera 3 with better spatial sampling.

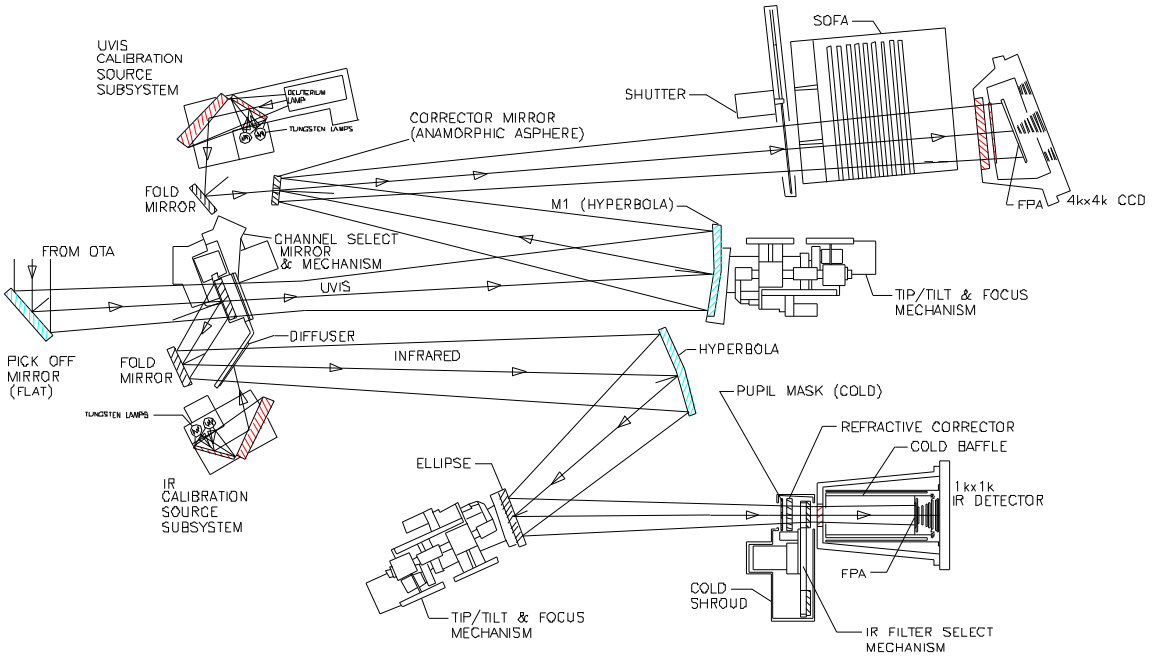

Figure 2. Schematic layout of the two-channel WFC3 instrument.

The instrument consists of two channels: the ultraviolet-visible WFC3/UVIS channel and the near-infrared WFC3/IR channel. Figure 2 provides a conceptual view of the WFC3 instrument. The pickoff mirror is a fixed element capturing light from the center of the HST focal plane and directing it into WFC3. The channel select mechanism is configured to direct light into either the UVIS channel or the IR channel. Each channel contains optics that provide correction for the HST Optical Telescope Assembly (OTA) spherical aberration, bring WFC3 to a common focus with the other HST instruments with a focus and alignment mechanism, and provide the required focal ratio at the detectors. The UVIS and IR filter elements are contained in selectable mechanisms. The design of the UVIS channel is based on elements from the ACS/WFC, with a 4096x4096 Charge Coupled Device (CCD) array covering a 160x160 arcsec field of view (slightly smaller than ACS/WFC and dictated by the size of the pickoff mirror). Since the UVIS channel is optimized in the UV-blue end of the spectrum, it will utilize aluminum mirrors with magnesium fluoride (MgF2) overcoats. Like WFPC2, it has a complement of 48 filters (see Figure 3 and Table 3 in Appendix 9), while ACS/WFC has 23, and STIS only 10. The WFC3 IR channel will house a 1024x1024 Mercury-Cadmium-Telluride (HgCdTe) detector array and has a FOV of 135x135 arcsec. Its optics – other than the Pick-Off Mirror (POM) - will utilize silver mirrors. To minimize internal background flux incident upon the HgCdTe detector, the detector and its surroundings (including the IR filter elements and a “cold stop”) will be contained in a cold enclosure. The IR channel accommodates 14 filters (see Figure 3 and Table 4 in Appendix 9). Both the UVIS and the IR channel include dispersive elements (prisms and grisms) for slitless spectroscopy.

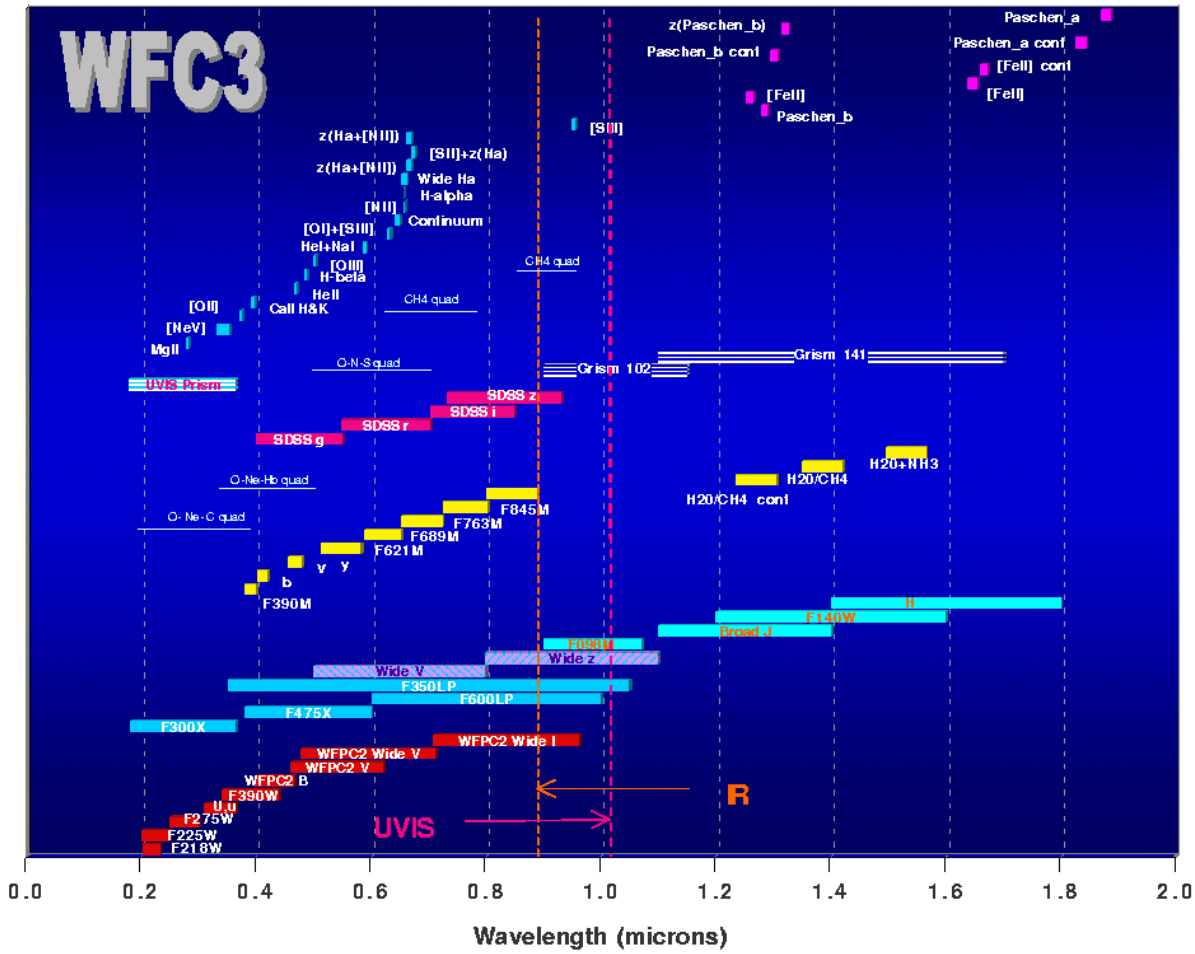

Figure 3: A schematic representation of the WFC3 filter set. The dashed vertical line marked "UVIS" indicates the UVIS channel long-wavelength sensitivity limit. The dashed vertical line marked "IR" indicates the IR channel short-wavelength sensitivity limit.

To compare the performance of HST cameras (apart from angular resolution), a useful index originally introduced by the ACS IDT is the "discovery efficiency," which is defined as the field of view multiplied by the throughput. In Tables 1 and 2 we tabulate the main characteristics and the predicted discovery efficiency of WFC3 compared to other HST instruments.

By using large-format CCD's, both WFC3/UVIS and ACS/WFC produce wide fields with spatial sampling of 0.040 and 0.050 arcsec respectively. These pixel sizes are comparable to that of the WFPC2 Planetary Camera (PC) channel (0.046 arcsec per pixel). However, WFC3 covers 20 times more field area than does WFPC2/PC and 25% more than WFPC2/WF. The WFC3/UVIS design offers a combination of excellent near-UV response and a large field of view (160 arcsec), giving it a discovery efficiency 12 times higher than any prior HST instrument at 3000 Å and 30

times higher than ACS/HRC. This effectively opens up for HST investigation a large new discovery space in the near-UV region.

Table 1: Characteristics of selected HST Imaging Instruments

Instrument	Wavelength Range (Å)	Pixel Size (arcsec)	FOV (arcsec^2)
WFPC2/PC	1200-10500	0.046	35 x 35
WFPC2/WF	1200-10500	0.100	3x 75 x 75
ACS/HRC	2000-10500	0.026	26 x 26
ACS/WFC	3500-10500	0.050	205 x 205
STIS/CCD	2000-10500	0.050	51 x 51
NICMOS/CAM2	8000-25000	0.076	19 x 19
NICMOS/CAM3	8000-25000	0.200	51 x 51
WFC3/UVIS	**2000-10500**	**0.040**	**160 x 160**
WFC3/IR	**8000-17000+**	**0.130**	**135 x 135**

Both the Wide Field and Planetary Camera 1 (WF/PC) and WFPC2 had relatively poor response at wavelengths below 3500 Å. Below 2500 Å, the low UV response exacerbated the problem of red leaks (i.e. unwanted long-wavelength photons) in the UV filters. STIS has much improved UV response, good resolution, and much reduced red-leak problem thanks to its Multi-Anode Microchannel Array (MAMA) detectors, but its imaging fields of view are very small (25 arcsec) and are not well matched to large, extended targets such as globular clusters, nearby galaxies, or distant clusters of galaxies. ACS/HRC (using a CCD) and ACS/SBC (using a MAMA detector) offer good response, but again over only small fields (26 arcsec and 30 arcsec, respectively). ACS/WFC has a large field of view but no sensitivity below 3500 Å (see Figure 4.)

WFC3 achieves its good near-UV performance by using aluminum mirrors coated with MgF2 and special blue-optimized antireflection coatings on its CCD detectors. HST is the only NASA-approved large-aperture mission with good UV performance. While NGST will provide higher sensitivity than any HST camera for wavelengths longwards of 6000 Å, its performance below 6000 Å is still not well defined and it is very likely that it will not perform at all shortwards of 4000 Å. In order to balance UV and IR capabilities it is important to have the best UV performance that can be provided for a reasonable cost.

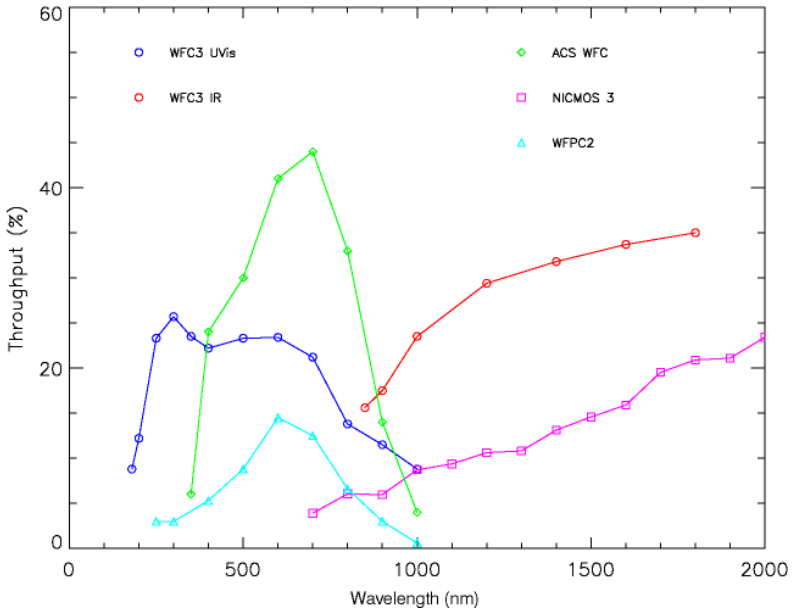

Figure 4. Comparison of the throughput of various HST imaging instruments. WFC3 has the highest throughput of all wide-field imagers both in the UV and in the near-IR.

WFC3's infrared channel will provide an important bridge spanning NICMOS and NGST. This can be achieved because WFC3/IR does not rely on expendable cryogens and thus is able to operate until the end of the HST mission. WFC3/IR will also become a workhorse for identifying objects of scientific interest for further study with NGST, SIRTF, and the large ground-based telescopes. Furthermore, WFC3/IR's good spatial sampling (0.13 arcsec per pixel versus 0.2 arcsec per pixel for NIC3) and larger field of view (135 arcsec vs 51 arcsec for NIC3) will provide an increased discovery efficiency of a factor of 15 in the 9000-17000 Å wavelength region compared to NICMOS (with the NICMOS Cooling System - NCS.)

Table 2 : Discovery efficiency of selected HST imaging. The 3000 and 6000 Å performance is normalized to that of WFPC2/PC, that at 16000 Å to NICMOS/Camera 2. The values for WFC3 are based on the baseline performance. Achieving the goal performance for WFC3 would double its discovery efficiency.

Instrument	**Discovery Efficiency**		
	@ 3000 Å	**@ 6000 Å**	**@ 16000 Å**
WFPC2/PC	1	1	N/A
WFPC2/WF	14	14	N/A
ACS/HRC	5.5	1.0	N/A
ACS/WFC	N/A	110	N/A
NICMOS/CAM2	N/A	N/A	1
NICMOS/CAM3	N/A	N/A	7.2
WFC3/UVIS	**180**	**36**	**N/A**
WFC3/IR	**N/A**	**N/A**	**105**

3.2 General WFC3 Scientific Priorities

Scientific programs for WFC3 naturally fall into two main categories:

(1) Extensions or continuations of imaging programs developed for WFPC2, ACS/WFC, ACS/HRC, and NICMOS;

and

(2) Programs which make use of WFC3's unique capabilities in the UV/IR or are particularly timely for the period 2004-2010. Examples of the latter are programs in support of and as follow-up to other major NASA and ground-based projects, including GALEX, SOFIA, SIRTF, 2MASS, the Sloan Digital Sky Survey (SDSS), and NGST.

Our discussion will focus primarily on scientific programs in the second category. Below we discuss the general potential of WFC3 imaging in the UVIS and IR channels separately, and then as a panchromatic camera covering the largest wavelength span of any HST instrument. In each case we will give a general overview of the capabilities and discuss in detail only a few selected programs aimed at illustrating the scientific potential of the instrument.

4. Ultraviolet Science

Although HST has achieved its long-heralded promise in the areas of high-resolution optical imaging and UV spectroscopy, its unique UV imaging capabilities have not yet been fully exploited mostly because of technical limitations. The low throughput, red leaks, and/or small fields of the UV imagers on HST to date have prevented users from exploiting quantitative UV imaging despite its great scientific potential. The UV spectral region is rich in information on the astrophysical properties of solar system objects, stars, star forming regions, and galaxies. The UV is, of course, uniquely sensitive to hot sources, in particular to the massive stars which are responsible for most "star-formation astrophysics," as well as to certain types of old, highly evolved, stars. This regime is also critical for studies of the metal abundances and surface gravities, two fundamental parameters of stellar astrophysics. Thus, the UV is the spectral region of choice for studies of the star formation and chemical enrichment histories of stellar systems, both in our own galaxy and others.

There are also many key diagnostics of interstellar gas and dust in the region below 4000 Å, including the 2175 Å peak in the dust extinction law, and a number of important emission lines such as the astrophysical plasma diagnostic emission line [O II] 3727 Å. However, neither STIS nor ACS offer good sensitivity over wide fields in the 2000-4000 Å spectral region.

For moderate and high-redshift objects ($z \geq 0.4$), the restframe far-UV ($\lambda < 1500$ Å) is redshifted into the 2000-4000 Å region in the observer's frame, making this a key probe of distant star-forming galaxies and active galactic nuclei (AGN). This near-UV region is particularly important in searching for galaxies in the $z \approx 1$-2 redshift range, based on "Lyman-dropouts." It is at these redshifts that the star-formation rate in the Universe might peak, according to estimates from deep surveys. Ground-based telescopes have great difficulty sampling this redshift range because the Earth's atmosphere is opaque to wavelengths below 3000 Å. Furthermore, the region 1600-2500 Å is one of the darkest parts of the natural sky background above the Earth's atmosphere, permitting the detection of extremely faint sources.

The combination of a large set of optical/UV filters, high sensitivity, high spatial resolution, low readout noise, low dark current, and large field of view will allow HST WFC3 to address a number of key scientific questions for the first time. A few important examples are described below.

4.1 Stellar Archaeology

(a) Resolved Stellar Populations

The history of star formation in galaxies is recorded in the types, or "populations," of stars they contain. HST's superb spatial resolution and ability to measure the brightness of individual faint stars in star clusters and nearby galaxies (see Figure 5) have enabled enormous strides to be made in our understanding of stellar mass distributions, and star-formation histories within our own

galaxy and nearby galaxies. WFC3 will significantly enhance the existing capabilities of HST in this area. Large, well-sampled fields of view are necessary to probe stellar populations in extended stellar systems. UV access is required for high-quality measures of stellar temperatures, metallicities, and surface gravities. For example, A and F type stars are particularly important for tracking metal enrichment, star formation histories, and galaxy disk evolution. The ability to obtain deep UV observations just shortward of the Balmer jump (3650 Å) provides an excellent estimator of surface gravities of these stars, thus providing information on their intrinsic luminosity.

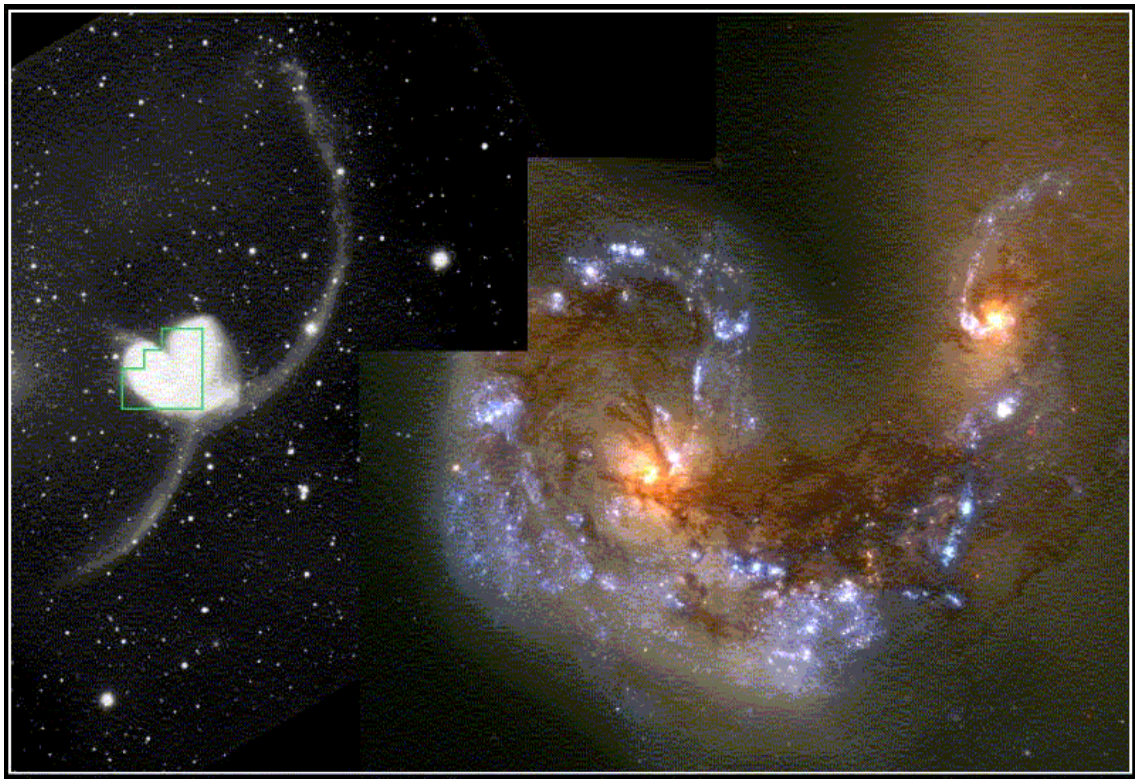

Figure 5. The Antennae Galaxies (NGC 4038/4039) imaged by WFPC2 (B. Whitmore and NASA). The image shows the richness of star-forming regions (rich in hot, young stars visible in blue) and dust lanes present in this merger of two spiral galaxies. The bulges of the merging spirals contain older, colder stars and are visible in red.

In older stellar populations (ages over 5 Gyr), helium-burning stars in advanced evolutionary phases have surface temperatures above 10000 K, making them UV-bright (see Figure 6). UV imaging by ASTRO/UIT and HST has recently opened up an entirely new window on this last under-explored corner of normal stellar evolution. These hot objects are not only important in their own right but also provide key information on mass loss during the red-giant-branch evolution which precedes the hot phases. Mass loss is a central problem in stellar astrophysics and is related to a number of other important processes, such as dust production, X-ray emission, and accretion flows in elliptical galaxies. We expect that the wide-field, near-UV capability of WFC3 will allow us to make rapid progress in increasing our understanding of advanced stellar evolution.

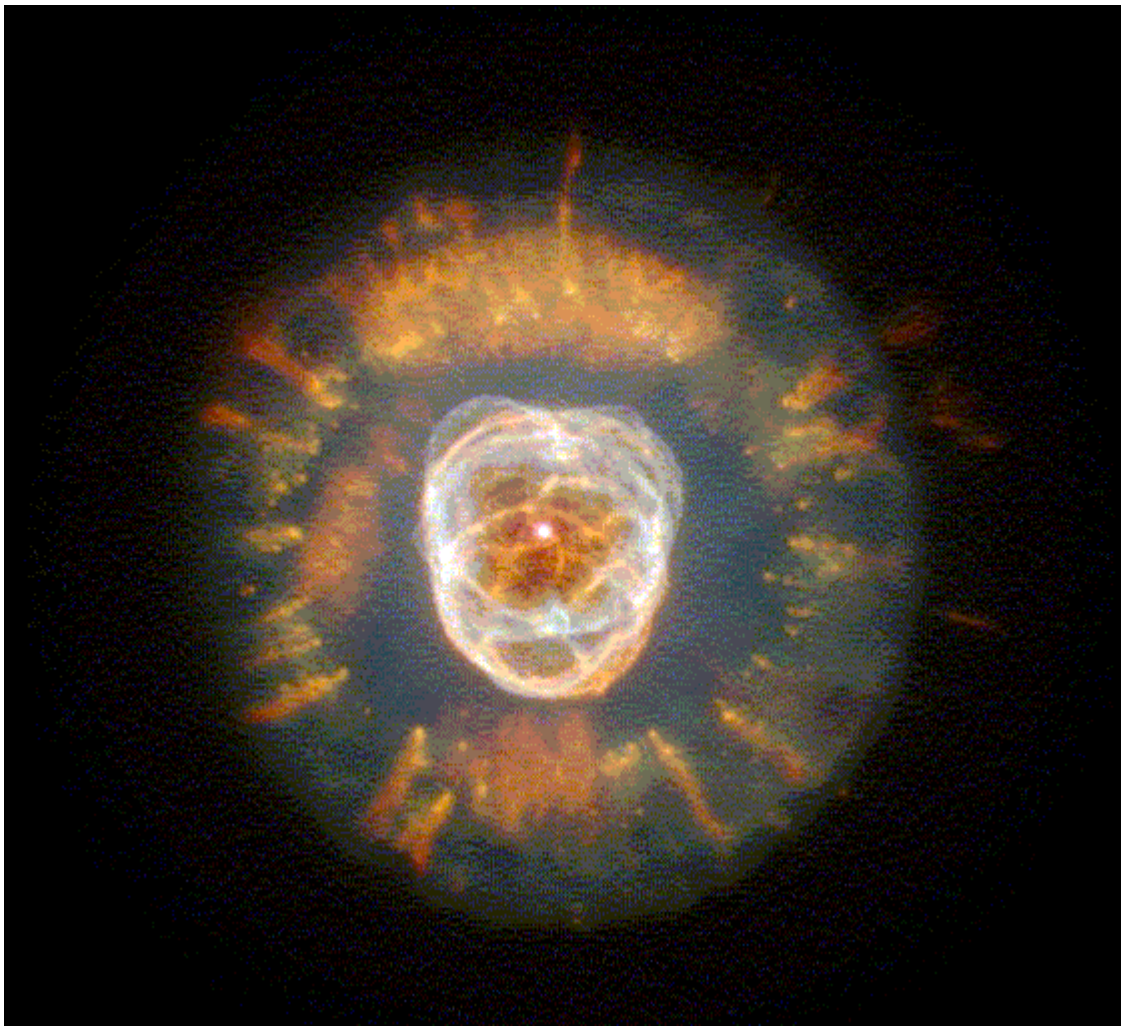

Figure 6. The Eskimo planetary nebula (NGC 2392) imaged by WFPC2 (A. Fruchter and NASA). The nuclei of planetary nebulae are old stars that have lost their outer layers and emit most of their light at UV wavelengths. This UV radiation ionizes the ejected material, producing the bright nebula.

(b) Stellar Populations in Integrated Light

For more distant galaxies, individual stars cannot be observed, but the constituent stellar populations can still be deduced from their integrated light. The ultraviolet sensitivity of WFC3 will be invaluable, since the ultraviolet has the highest sensitivity of any spectral region to stellar temperature and metal abundance. These are the types of parameters needed to deduce stellar populations, star-formation rates (SFR's), and star-formation histories. Figure 7 illustrates the strong evolution of the integrated UV energy distributions of stellar populations over timescales up to 3 Gyr. The spectra in the figure have been normalized at 5500 Å (the V band). The amplitude of the spectral change at 2000 Å is over 4 magnitudes larger (a factor 40 in flux) than the change at 10000 Å. Furthermore, the figure shows that the spectral line structure of the region shortward of 5000 Å contains a wealth of information which can be analyzed with narrow- and intermediate-

band filters. The high-sensitivity region begins below about 4000 Å, where the confluence of hydrogen absorption lines in hotter stars and the Balmer Jump and metallic absorption features in cooler ones begin to strongly affect the gross spectral structure.

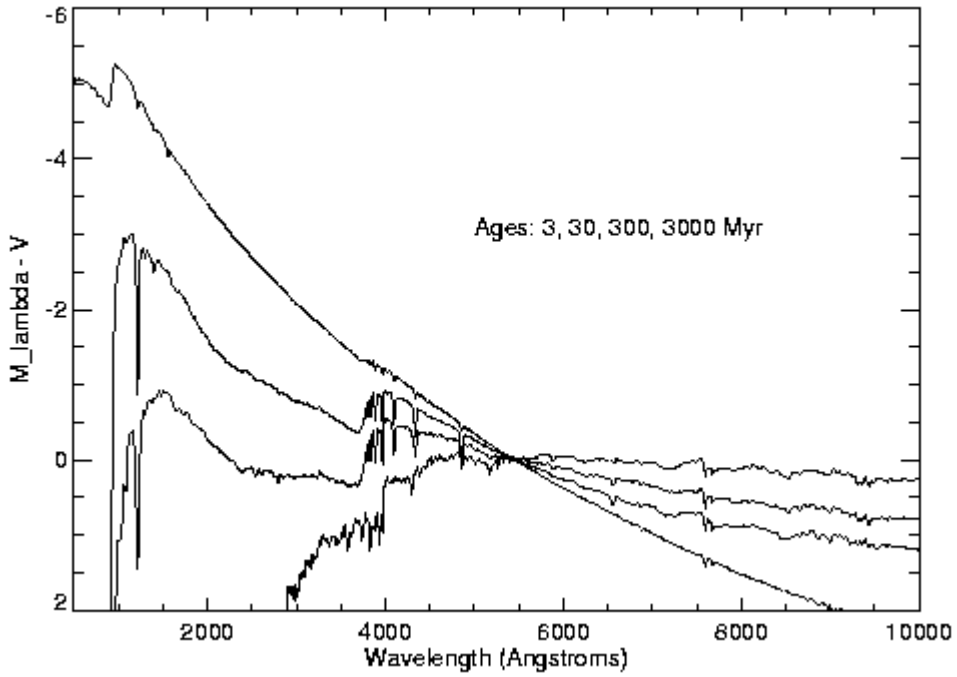

Figure 7. Theoretical model spectra of integrated stellar populations of various ages. We plot the magnitude as a function of wavelength normalized to the visible band. The spectra become redder with increasing age (G. Bruzual and S. Charlot 1996).

The UV allows *direct detection* of the massive stars responsible for most of the ionization, photo-dissociation, kinetic-energy input, and element synthesis in galaxies. These processes are responsible for much of the astrophysics of the universe. By contrast, most other methods of studying massive star populations yield only *indirect* measures since they rely on re-processing of the UV photons by the surrounding medium (H II regions or dust clouds). Furthermore, since the production of Lyman-continuum photons by young populations rapidly declines after ≈ 5-10 Myr, these other methods probe star formation only over a short period, which constitutes a tiny fraction (0.05%) of the lifetime of a galaxy. By comparison, the short-wavelength continuum below 4000 Å remains a sensitive indicator of star-formation histories for ages up to 100 times greater.

4.2 The Assembly of Galaxies at High Redshift

We now suspect that much of the "final assembly" of galaxies, and much of the conversion of primeval gas into stars, occurred at relatively low redshifts in the range z ≈ 1-3. These redshifts

correspond to lookback times of half to three-quarters of the present age of the Universe. The most productive technique developed so far for identifying star-forming galaxies in this redshift range and greater is the "Lyman-dropout" method, which uses the fact that absorption from the ground state of neutral hydrogen produces a strong discontinuity in the restframe energy distribution below 912 Å. Unfortunately, the Lyman-dropout technique is not applicable to most of this redshift range, unless one has access to the observed wavelength interval 2000—3500 Å. The wide field and good near-UV sensitivity of WFC3 are ideally suited to the exploration of this critical early epoch.

WFC3's enhanced sensitivity over WFPC2 will permit identification of candidate sources in the more distant ($z \approx 3$-5) range up to 2 magnitudes fainter than achieved in the Hubble Deep Fields. At present, our sample of these distant objects is limited to only the most luminous young galaxies. The WFC3 U and B band dropout sample – obtained by searching for galaxies lacking flux in the U- and the B-band, respectively, but which have relatively bright luminosities at longer wavelengths - would be a basic resource for spectroscopic campaigns by the NGST.

One can also exploit the hydrogen Lyman-alpha emission line (1216 Å in the rest frame), which has been found to be bright in many distant galaxies. This feature can be detected with narrow-band filters or prisms in the 2000-5000 Å range, covering redshifts $z \approx 0.8$-3. Of special interest are the numerous "sub-galactic clumps," which make up a significant part of the faint blue galaxy population. Through the process of repeated hierarchical merging, it is believed that these clumps came together to form the luminous galaxies we see today, i.e. they are the building blocks of galaxies. If they exist everywhere, they may be used to trace the large scale structure of the Universe. Hence the statistical and physical properties of these objects are essential in order to constrain theories of galaxy formation.

A final, more speculative possibility for WFC3 is the detection of very high redshift ($z \approx 10$) systems with hard intrinsic extreme-UV energy distributions - redshifted into the 2000-4500 Å region. Absorption by the surrounding neutral hydrogen usually extinguishes sources in the restframe spectral region between ≈ 600 and 912 Å. However, sources with a sufficiently hard intrinsic extreme-UV continuum will become bright again at shorter EUV wavelengths. Such objects will have very peculiar colors in broadband optical/UV imagery, and the UV-blue bandpass for which WFC3 is optimized is ideally suited to search for these. Such techniques might be able to identify the first generation of active galactic nuclei.

5. Near-Infrared Science

The WFC3 infrared channel has unique and powerful capabilities in the 0.8-1.7 μm spectral region. HST, even with a relatively warm optical system, offers four key advantages for near IR imaging over much larger ground-based facilities:

- continuous coverage of the 0.8-1.7 μm wavelength range, unaffected by the atmospheric water vapor absorption which mutilates ground-based data;
- a reduction by nearly 3 orders of magnitude in the sky background emission shortwards of 1.7 μm (due primarily to atmospheric OH bands);
- the ability to have stable, uniform, near diffraction-limited imaging over a large field of view (135×135 arcsec with WFC3);
- stable and accurate photometry over a large field of view compared to the small isoplanatic patch and variable point spread function available to ground-based adaptive optics (AO) systems.

Such a potent combination of performance characteristics is impossible to achieve from the ground and makes the near-IR capabilities of WFC3 compelling.

In the design of WFC3/IR it was decided not to cover wavelengths out to the 2.5 μm cutoff of NICMOS. This compromise allows the WFC3 near-IR detector to be cooled simply by thermo-electric coolers, rather than by expendable cryogen or a mechanical cooler. The fact that WFC3-IR does not extend to the K band (2.2 μm) is not a serious limitation, since the HST Optical Telescope Assembly (OTA) itself generates a significant background at K, while adaptive-optics systems on large ground-based telescopes optimized for IR performance will become very competitive in the K band during this decade. On the other hand, the reduction in the H band (1.6 μm) sky background in space renders HST near-IR imagers more sensitive than similar instruments on 8-meter class ground-based telescopes, even with sophisticated adaptive-optics systems. Thanks to the use of more modern detectors, WFC3 improves on the discovery efficiency of NICMOS by more than a factor of 15. Below we have singled out a few examples from the many programs that are made possible by WFC3/IR.

5.1 The Highest -Redshift Galaxies

Deep observations with HST and ground-based telescopes demonstrate that there are hundreds of thousands of faint, distant galaxies per square degree of sky. Because spectroscopic integration times are long, even for ground-based telescopes in the 8-m to 10-m class, it is essential to employ efficient survey techniques that can isolate the objects of greatest interest for various astrophysical investigations. As we have already discussed, the most productive technique for identifying high-redshift, star-forming galaxies is the "Lyman-dropout" method, which at low redshift relies on the Lyman discontinuity at 912 Å. As the redshift increases, the effect of absorption due to intergalactic neutral hydrogen clouds – known as the *Lyman-α forest* - moves the rest-frame wavelength of the continuum drop from the Lyman limit at 912 Å up to the Lyman α at 1216 Å. Both discontinuities can be detected readily in multiband imaging. This method has been used with both ground-based and HST imaging to identify candidate galaxies in the $z \approx 3$-5 redshift range, and will most likely be the technique for providing us with the first large samples of objects beyond redshift 5. WFC3/IR can open new territory to this method, and - thanks to its sensitivity and field of view - achieve real breakthroughs in the search for the highest-redshift galaxies. In particular, a problem that WFC3/IR can tackle is that of constraining the so-called re-ionization epoch of the Universe. This is the time when the neutral gas permeating the Universe since the release of the cosmic microwave background - at redshift above 1000 - becomes ionized again and thus transparent to Lyman-α light. According to some recent models, this epoch, known to cosmologists as the *End of the Dark Ages*, should occur at a redshift between 6 and 10. For galaxies at redshift 7 through 10 the Lyman break will occur at 1-1.3 μm and appear as I or J band dropouts (see Figure 8). They will be identified by deep I, J, and H band deep observations. Since the search must be carried out with high sensitivity over a wide field in the near-IR and because high-redshift galaxies are generally very compact (<0.2 arcsec in size), ground-based facilities will not be competitive with WFC3/IR for this particular project. WFC3/IR will be in a position to verify the model predictions and, if they are correct, to see the first objects shining through the Universe. Depending on their nature, WFC3/IR may even detect the objects responsible for the re-ionization itself.

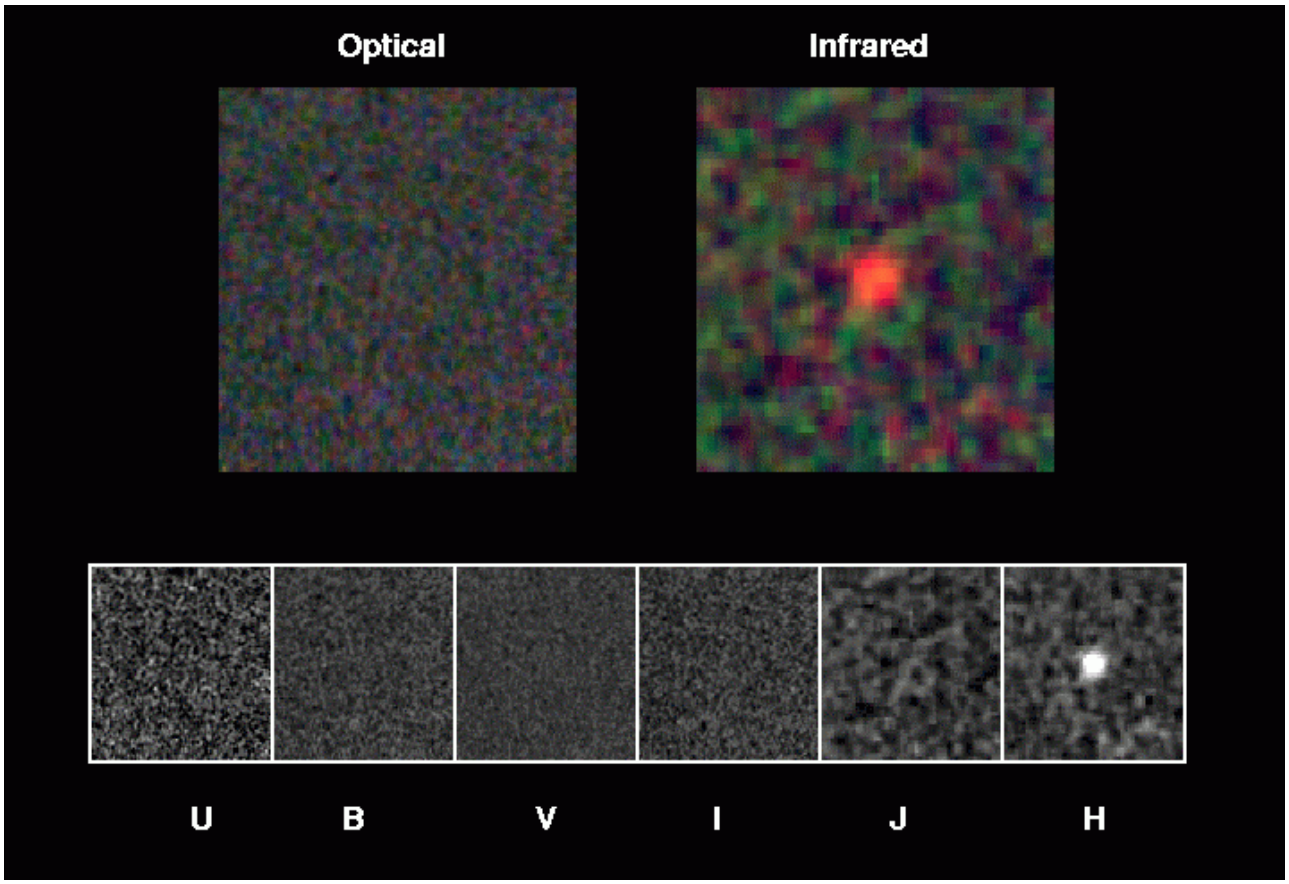

Figure 8. J-dropout object identified in the Hubble Deep Field North. This object is visible only in the NICMOS F160W (H) image. The U, B, V, and I images were obtained with WFPC2, the J and H images with NICMOS. Similar objects could be found in large numbers by WFC3 by searching a large area for sources bright in the H band and faint in the J band (M. Dickinson).

5.2 Water and Ices on Mars and the Outer Planetary Satellites

Despite three and a half decades of Mars exploration, a great deal of uncertainty remains over the amount, disposition, and variability of water vapor in the planet's atmosphere and its relation to subsurface ice, hydrated minerals, and other volatiles. WFC3 offers the prospect to measure Mars' atmospheric water vapor with spatial resolution down to a few tens of km with a filter designed for the 1.4 μm water-vapor band (see Figure 9). The spatial resolution and sensitivity to small spatial and temporal changes in water vapor measured in this way exceeds the capabilities of ground-based telescopes by a wide margin. Given the requirements on spatial resolution, minimal scattered light, and the fact that 1.4 μm is in the center of the Earth's atmospheric water band, observations such as these are possible only from space. Observations with HST complement *in situ* measurements with spacecraft since the latter can only carry out local measurements and are less well suited to follow seasonal variations in the Martian atmosphere water vapor content.

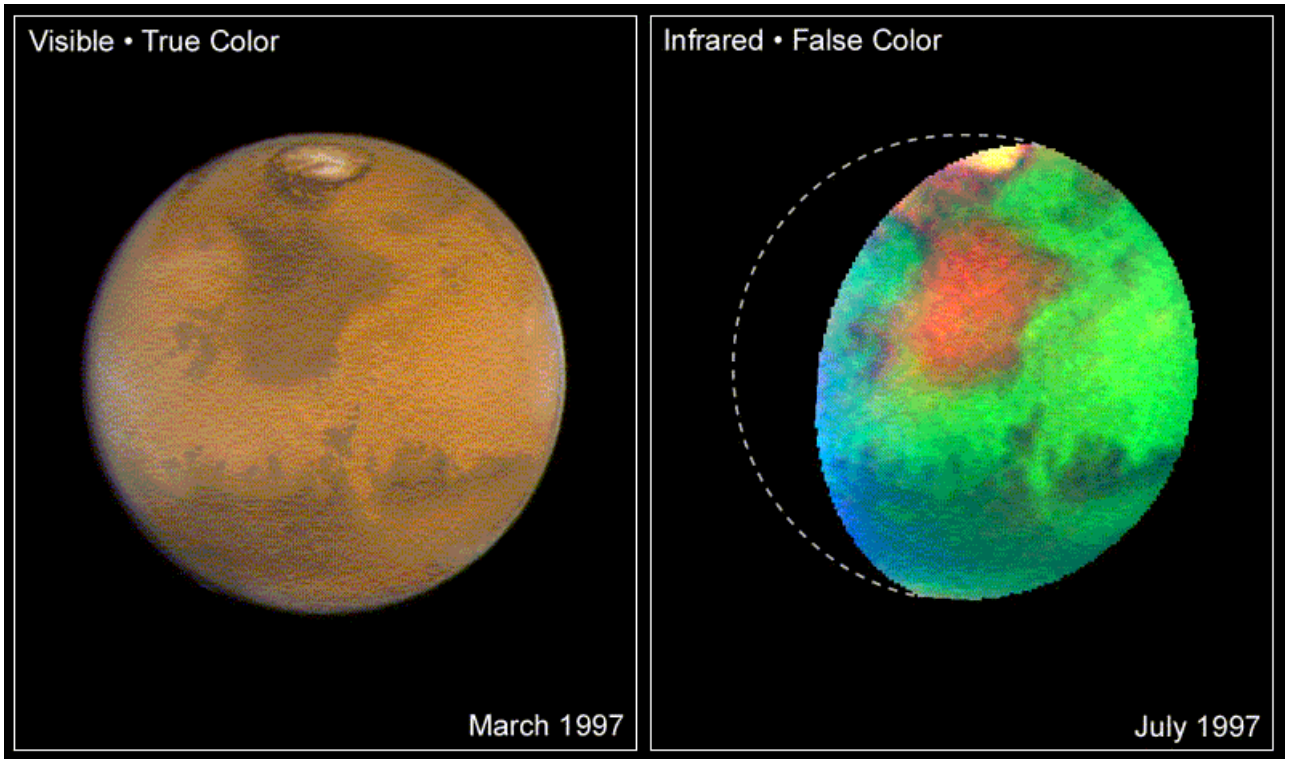

Figure 9. Water in Martian rocks as revealed by WFPC2 (left panel) and NICMOS (right panel) observations. The bluer shade along the edges of the Martian disk in the left panel is due to atmospheric haze and water ice clouds. The large reddish region in the right panel identifies an area of water-rich minerals known as Mare Acidalium (J. Bell, J. Maki, M. Wolff, and NASA).

The surfaces of many of the satellites of the outer solar system planets have long been known to retain ice. Because temperature declines with distance from the Sun, the dominant type of ice varies with solar distance, from H_2O in the satellites of Jupiter and Saturn, to CH_4 (Uranus) and CO and N_2 (Neptune's Triton). It is likely that additional ices await discovery on the surfaces of satellites from Jupiter to Neptune, and there is a possibility for major surprises. The most spectrally active ices, for example, are not necessarily the most abundant ices. Methane on Pluto was once thought to be a dominant constituent, but is now recognized to be only a small contaminant of nitrogen, the truly dominant constituent. Ground-based data suffer from inadequate signal-to-noise ratio and from errors due to subtraction of the scattered-light background from the adjacent planets. This is especially true of the faint, inner satellites (e.g. JV, JXIV, S15, U7) for which no suitable near-IR spectra exist. The low scattered-light background of HST will allow the first high-quality near infrared (slitless) spectra of many planetary satellites. Of particular value will be WFC3's continuous coverage from 0.8 to 1.7 μm.

6. Panchromatic Science

The information on astrophysical sources contained in each of the UV, visible, and near-IR bands is strongly complementary to the other bands, since each band is affected differently by hot stars, cool stars, and dust. Emission and absorption lines suitable to probe in detail the physical properties of stars and the interstellar medium are found throughout this broad wavelength interval. Moreover, the redshifts of distant galaxies move important spectral features, located at short wavelength in their rest frame, into the observer's infrared band. At least one of the two most important features in the continuum of composite stellar populations – the Lyman break and the 4000 Å break – will be found within the wavelength range of WFC3 for redshifts throughout the range 0 through 12: an enormous volume of the Universe. For these reasons, many scientific programs would greatly benefit from a wavelength coverage from the UV to the near IR, the interval for which WFC3 is being designed.

There is another factor that makes the panchromatic WFC3 compelling. The two extremes of the WFC3 sensitivity interval correspond to minima in the zodiacal sky background generated by optical scattering of sunlight and IR emission by the dust particles in the plane of our solar system. The peak in zodiacal background occurs in the 5000-7000 Å region. On either side of this, however, there are very dark minima lying at 2000 Å in the mid-UV and at 3 μm in the near-IR. The HST OTA thermal emission shifts the minimum background wavelength in the infrared to 1.6 μm. In these deep windows the background is 40-100 times fainter than at any wavelength at the finest ground-based sites. It is also over 10 times fainter than the sky from HST orbit at wavelengths of 5000-7000 Å. With its panchromatic coverage, WFC3 is well suited to take advantage of both the UV and IR dark windows in observations of low-surface-brightness extragalactic objects. Applications include the study of faint circum-galactic regions in nearby galaxies (e.g. tidal streams), intergalactic clouds, dwarf galaxies, and galaxies and proto-galaxies at high redshifts (for which the surface brightness scales inversely as the fourth power of the redshift). Objects that have surface brightness up to 1000 times fainter than can be detected with ground-based telescopes will be identifiable with WFC3.

In the following subsections we discuss the contributions that the panchromatic capabilities of WFC3 will allow in three broad areas of astrophysical research.

6.1 Galactic Evolution

The most powerful insights into galaxy evolution will emerge from a *panchromatic* approach which combines the special features of the UV, optical, and IR spectral domains. Together, these offer the best probes of normal stellar populations and medium-temperature interstellar gas. These are the primary domains for galaxy astrophysics, without which the insights offered by other spectral bands (such as radio, far-infrared and X-ray) on very cold or very hot material are incomplete.

The power of panchromatic imaging to "dissect" the structure of galaxies is illustrated in Figure 10, which compares a 2500 Å image of the nearby spiral galaxy M81 to a normal R-band (6500 Å) image. Early-type spirals like M81 and barred galaxies tend to exhibit the largest morphological changes with wavelength. In the left panel of Figure 10 the UV morphology of M81 would be classified with a Hubble galaxy type dramatically different from that derived from its visible band morphology. The optical bulge is dominated by cool main-sequence and giant-branch stars, and it dims progressively at shorter wavelengths. By contrast, hot OB stars in the spiral arms increase in brightness in the UV so that the arms stand out. The UV images permit analysis of star-formation physics through detailed comparisons of massive star formation over the past few 100 Myr to the distribution of hot and cold interstellar gas (e.g., as measured by Hα emission and radio-band neutral hydrogen maps).

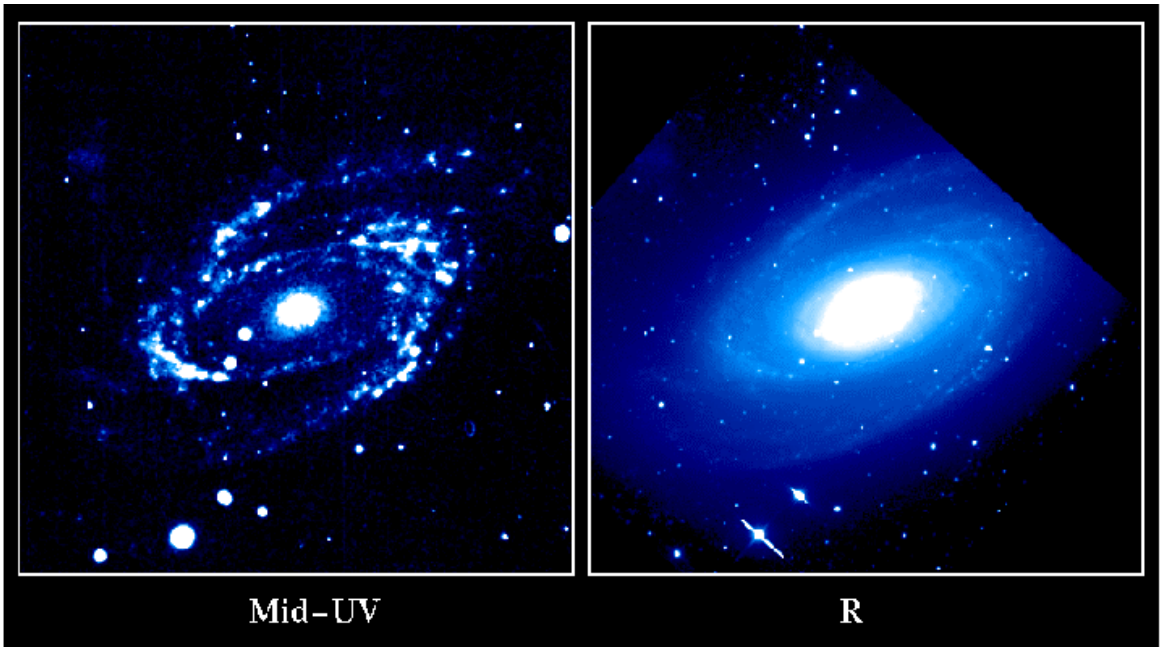

Figure 10. Images of the nearby spiral galaxy M81 at 2500 Å (from the Astro/UIT, left panel) and in the R band (6500 Å) right panel. The central bulge is dominated by cool main sequence and giant branch stars, and it progressively diminishes at shorter wavelengths. By contrast, hot OB associations in the spiral arms increase in brightness in the UV so that the arms stand out (R.W. O'Connell.)

In contrast to the UV, the near IR H band (1.6 μm) flux is mostly sensitive to stellar mass, with little dependency on age and metallicity (see Figure 11.) Multiband imaging from the UV to the near IR allows one to correct for the omnipresent effect of dust obscuration, e.g., by using the so-called dust-insensitive color combinations. Panchromatic UV-to-IR imaging of nearby normal galaxies also serves as a basis for interpreting galaxies at high redshift. The rest-frame UV continuum is measurable to very high redshifts ($z \geq 10$) with instruments like NGST and serves as a key index of the cosmic star-formation density as a function of time. Panchromatic images of nearby galaxies are also necessary to calibrate the large "morphological K-correction" which arises

because of the strong changes in galaxy appearance with rest wavelength. This must be quantified in order to distinguish genuine evolutionary effects from simple band-shifting. For example, M81 (Figure 10) has an almost ring-like appearance in the UV. A high-redshift version of M81 observed in the restframe UV might be mistakenly interpreted as a short-lived, non-equilibrium system rather than the stable structure we know it to be.

With multiband WFC3 exposures, astronomers will make important strides in understanding the astrophysical drivers of galaxy UV luminosities, the cosmic star-formation history over the past few Gyrs, and the nature of the strange systems detected at high redshifts.

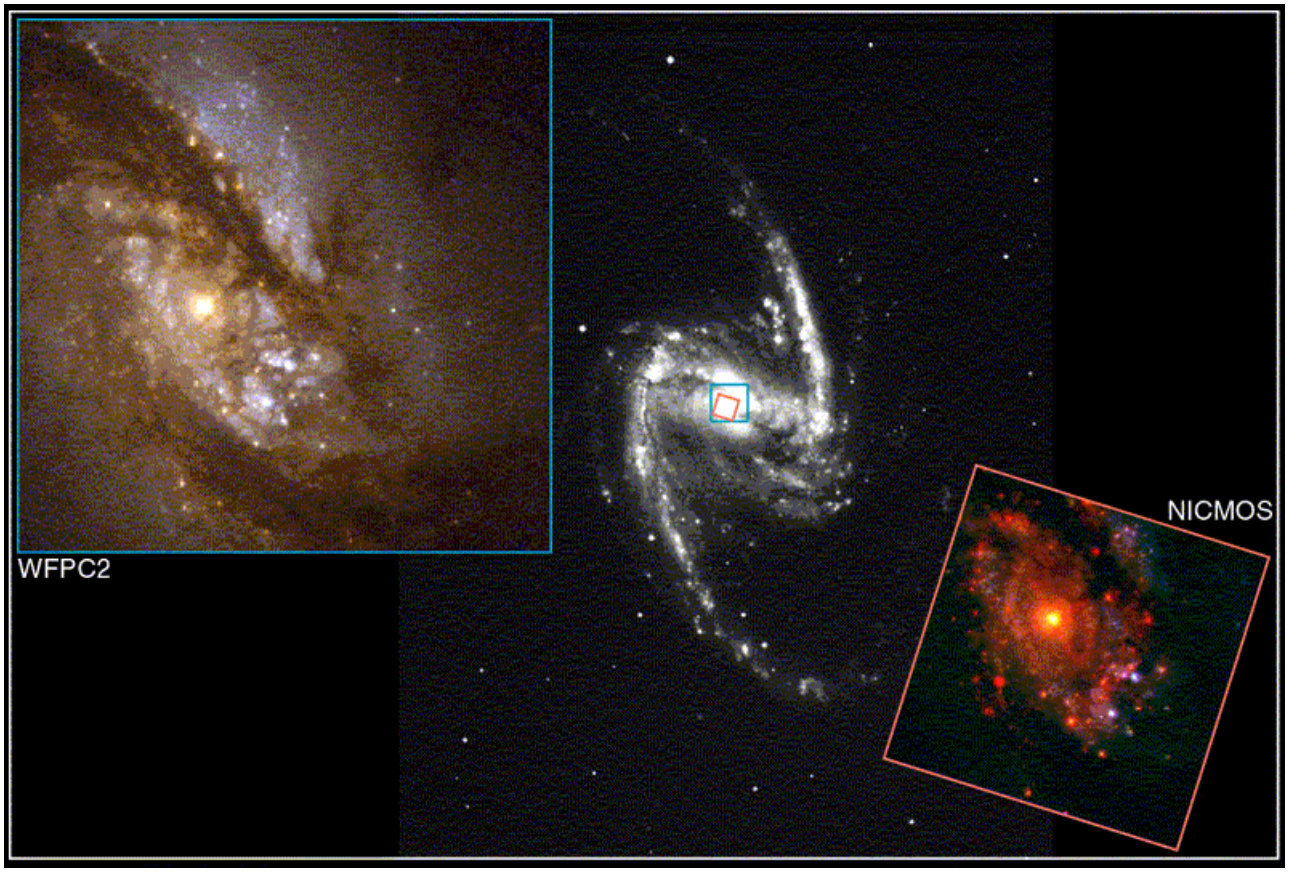

Figure 11. The nucleus of the active, star-forming galaxy NGC 1365 imaged with WFPC2 (upper left inset) and NICMOS (lower right inset) and from the ground (central image). Some of the star clusters visible in red in the NICMOS image are enshrouded in dust and undetectable in the WFPC2 images. The infrared image traces the intrinsic stellar mass distribution better than the visible light image. The bright source at the center is the active nucleus (M. Carollo and NASA).

6.2 Star Birth, Death, and the Interstellar Medium

Images of gaseous nebulae obtained by HST's WFPC2 are as astounding to experienced astronomers as they are to the general public. WFPC2 exposed the processes by which stars form in the dense cores of cold, dusty, and dark molecular clouds, why stars form prodigiously in some galaxies but not in others, and how they end their lives by shedding their outer layers. WFC3 is a fitting legacy of WFPC2. The difficult questions posed by WFPC2 will be attacked in detail by WFC3, providing new images that will form the basis of research long past the decommissioning of HST in 2010. WFC3 extends the spectral coverage as well as the sensitivity of WFPC2, and adds a host of important new filters for new types of scientific investigations.

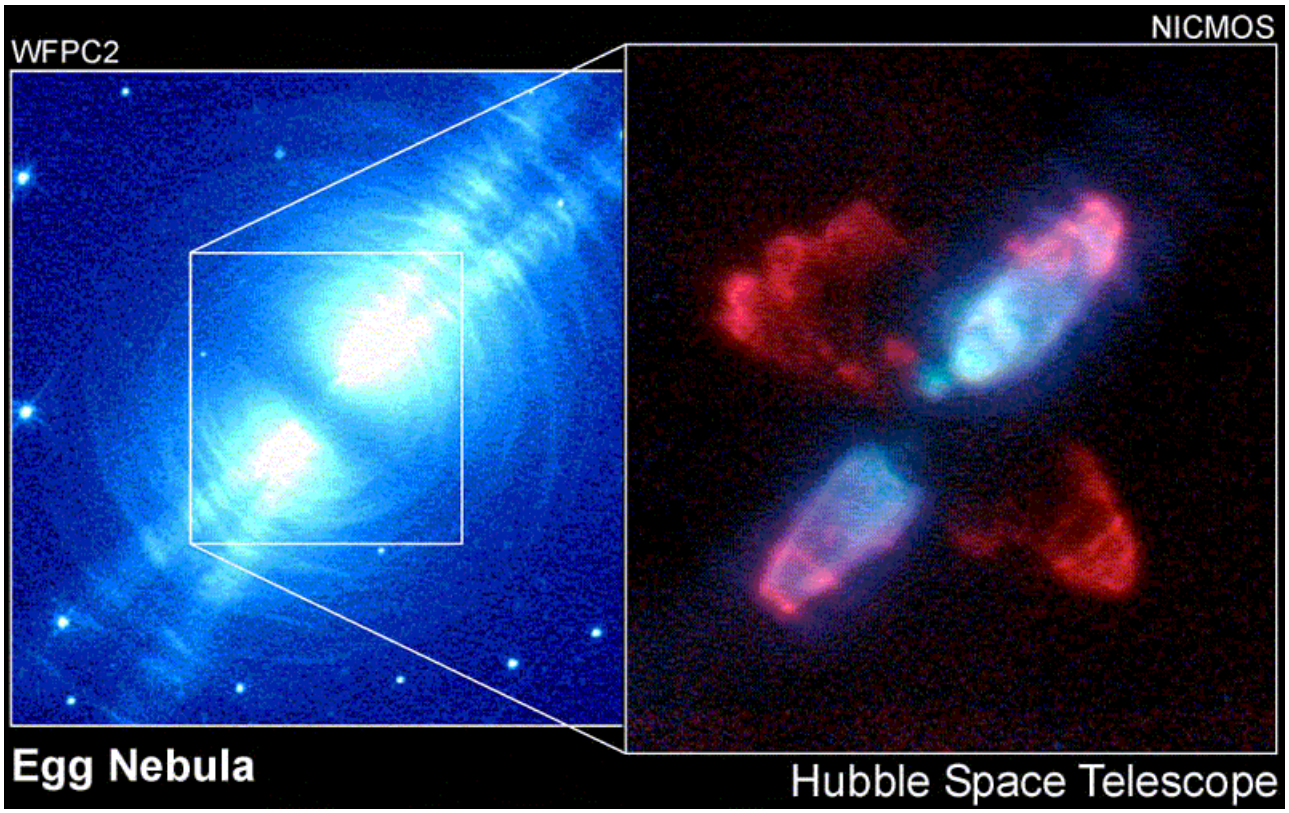

Figure 12. WFPC2 (left panel) and NICMOS (right panel) images of the Egg Nebula (R. Thompson, D. Hines, R. Sahai, and NASA). The NICMOS image is color coded. The red features correspond to emission from hot ionized gas, the blue features to starlight reflected by dust.

(a) Stellar Outflows

WFC3 will be used to measure the physical, chemical, and ionization structures in the powerful winds emitted by both young and old stars, such as T Tauri stars, luminous blue variables, Herbig-Haro objects, Wolf-Rayet bubbles, planetary nebulae (see Figures 12 and 14), and novae.

Infrared images are necessary to probe heavily reddened objects with strong scattering. These studies will allow us to connect the births of stars to their surroundings, and to see how dying stars stir up and enrich the inter-stellar medium with their winds. Direct imaging in the 1.64 μm [Fe II] line with WFC3 will allow observers to probe winds in young stars down to the scale of our solar system, which should constrain possible formation mechanisms.

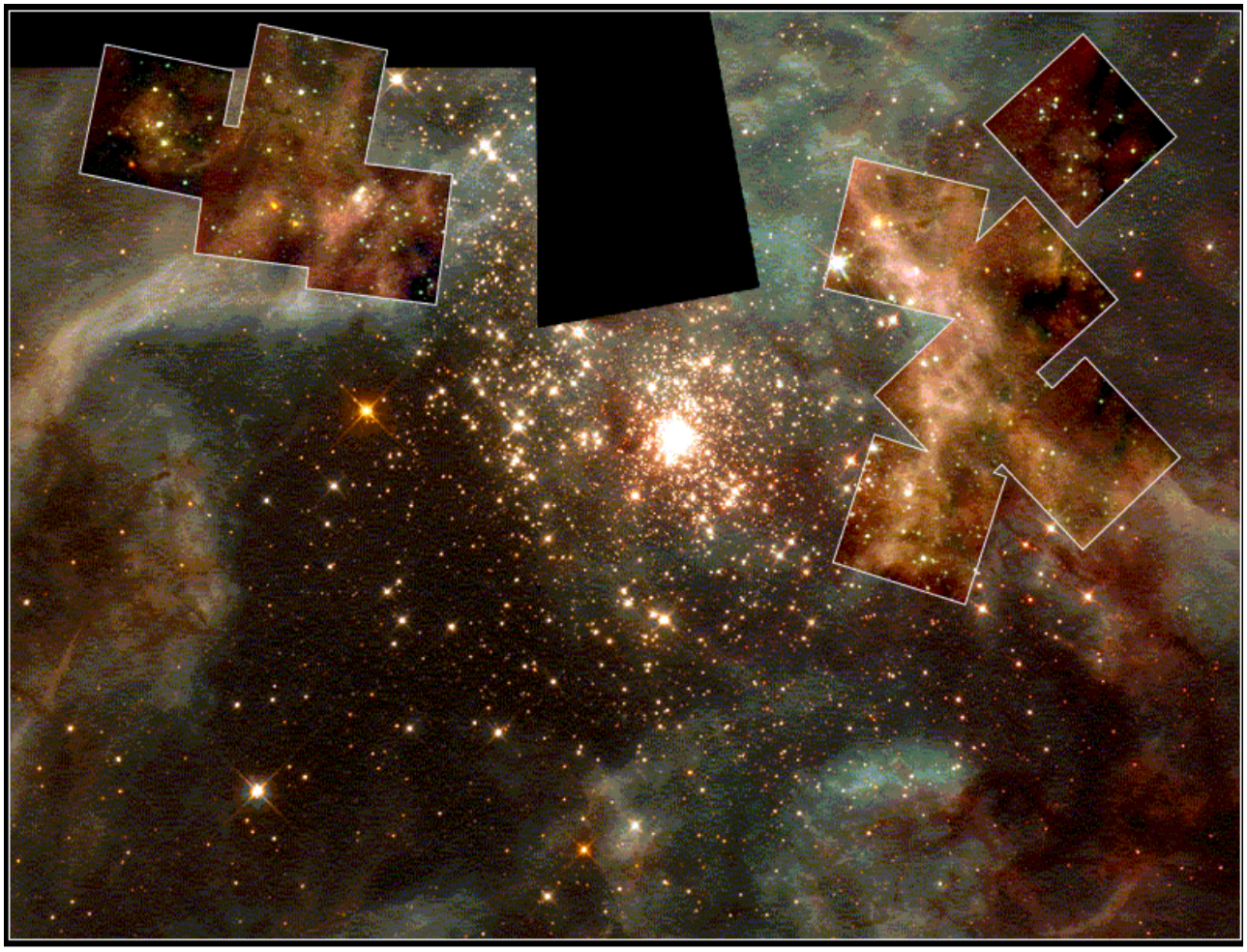

Figure 13. Composite WFPC2 (background image) and NICMOS Camera 2 mosaics (smaller insets) of the 30 Doradus Nebula in the Large Magellanic Cloud (N.Walborn, R. Barba and NASA.) The NICMOS images allow us to study the dust-enshrouded star-formation triggered by the bright star cluster visible in the WFPC2 image. The IR channel of WFC3 would allow us to cover the whole area shown with just two exposures instead of the 10 used to get partial coverage with NICMOS Camera 2.

(b) Initial Mass Function

Near-infrared imaging with the HST offers unparalleled opportunities to cut through surrounding dust cocoons (see Figure 13) to measure the initial mass function to below the hydrogen-burning limit in different galactic environments. WFC3's sensitivity to the infrared water vapor and methane features that are characteristic of the lowest-mass stellar and sub-stellar objects provides a powerful capability for studying low-mass stars and brown dwarfs. The important water feature is unobservable from ground-based facilities because of the strong absorption by the Earth's atmosphere. These studies may help us to understand the origin of the similarities and differences in the initial stellar mass function throughout the Milky Way and nearby galaxies.

(c) Formation of Planetary Nebulae

Using WFC3, astronomers will obtain critical data on the mass ejection that ordinary stars like our Sun undergo as their lives end. These stars eject their outer layers in beautiful and intricate patterns (see Figures 12 and 14) that were never predicted by the otherwise highly successful models of stellar evolution. WFC3's panchromatic cameras will provide much improved temperature, composition, and density probes of such planetary nebulae. Motions of HST-resolved small emission knots caught up in the flow like tracer particles permit us to determine distances to these objects and their dynamics with much better accuracy.

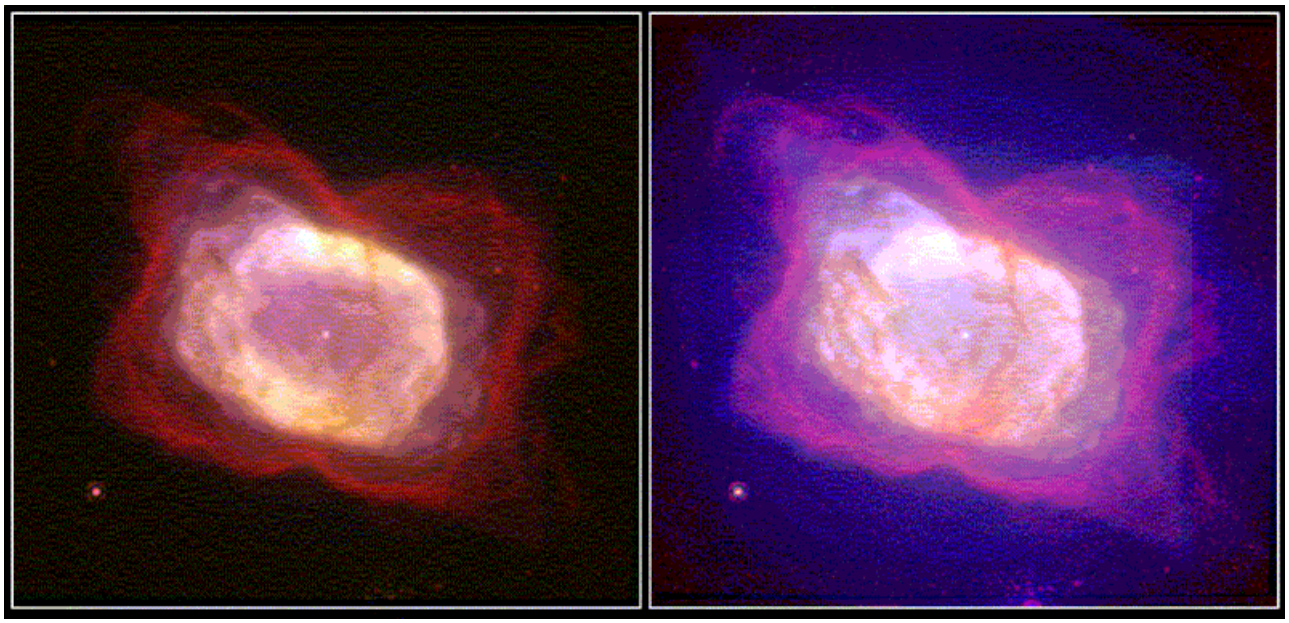

Figure 14. The planetary nebula NGC 7027 imaged with NICMOS (left panel) and NICMOS plus WFPC2 (right panel). In the left panel the red color represents cool molecular hydrogen, the white area represents gas ionized by the central star. In the right panel, in addition to the ionized gas (white) and the molecular gas (pink and red), the area where the star light is reflected off dust is visible in blue (W. Latter and NASA).

(d) Physical Structure of Galactic Nebulae

WFC3 will be used to investigate the small-scale ionization structure of Galactic nebulae (Figure 15.) The physics of these objects is largely determined by hydro-dynamical and radiative-transfer effects with characteristic scalelengths of order 10^{15} – 10^{16} cm which, for nearby nebulae,

correspond to typical angular scales of 0.1 to 1 arcsec. Examples include the structure of ionization and shock fronts in H II regions, supernova remnants, and stellar outflows. Understanding the physics of these structures underlies interpretation of a wide range of astrophysical phenomena. The improved quantum efficiency and sampling of the WFC3 CCDs relative to the WFPC2, together with the availability of a more comprehensive wide-field narrow-band capability than offered by ACS, will make the WFC3 the premier instrument on HST for this work.

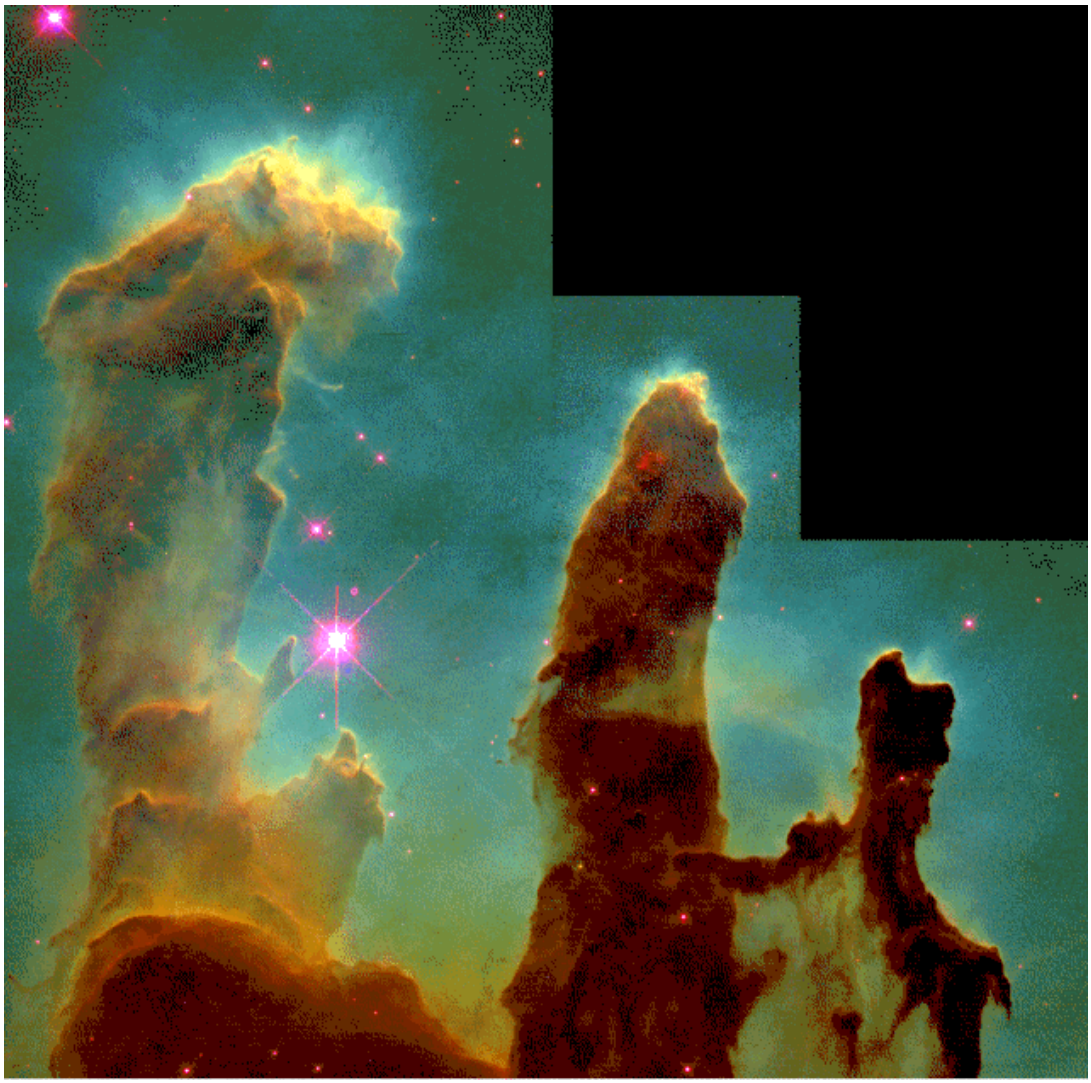

Figure 15. WFPC2 image of the galactic nebula M16. The image shows low-ionization sulfur emission ([S II]) as red, hydrogen recombination emission as green, and high-ionization oxygen ([O III]) emission as blue. The image emphasizes the small-scale structure that dominates much of the physics of the interstellar medium (J. Hester and NASA.)

(e) Young Stellar Objects and their Surroundings

WFC3 will probe deeply into interstellar molecular clouds where stars are born and investigate the surroundings of young stars as they form and evolve. The infrared emission, both from atomic and molecular tracers and from dust-scattered starlight, can escape from the cloud and be detected, whereas visible light is essentially completely absorbed (Figure 16.) Certain zones at which winds from the collapsing star batter the gas around them can be uniquely mapped using the diagnostic lines of [Fe II] line at 1.64 μm.

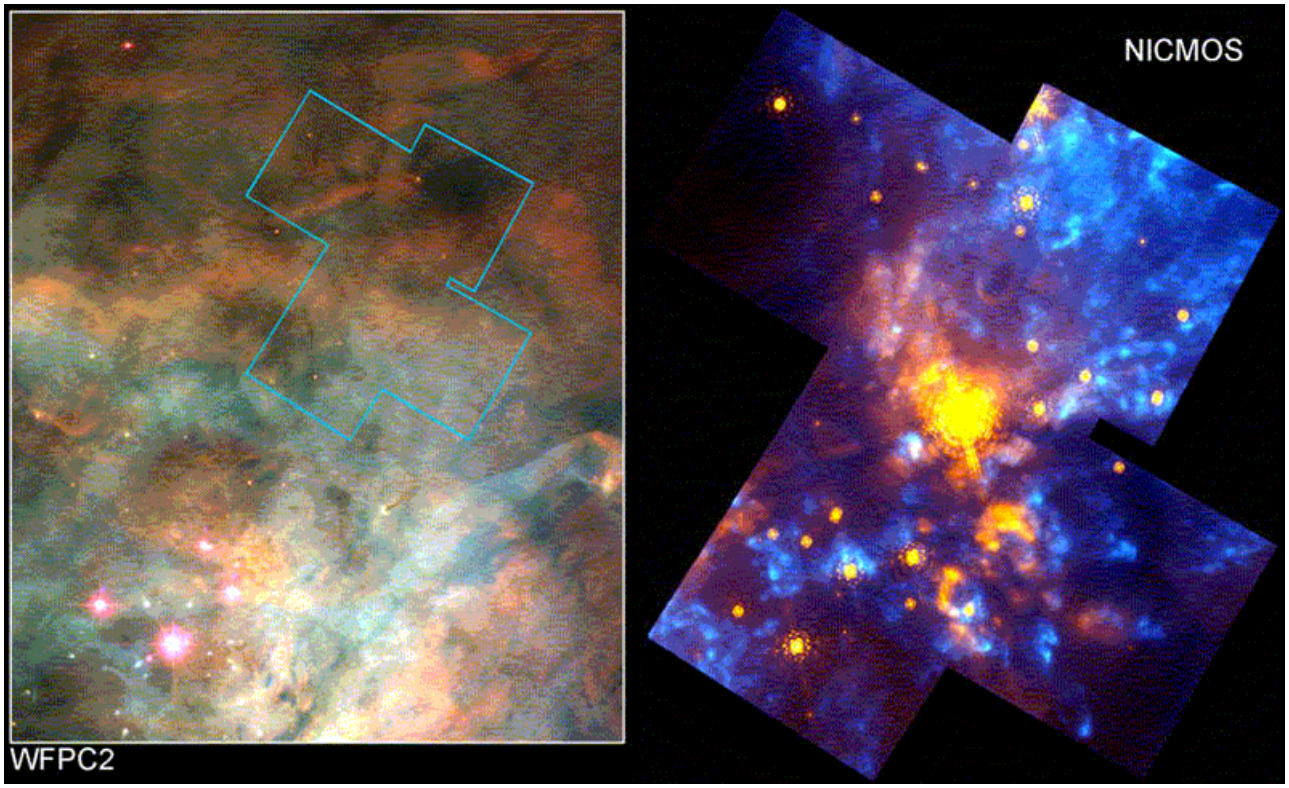

Figure 16. A region in the Orion molecular cloud OMC-1 imaged by WFPC2 (left panel) and NICMOS (right panel). In the NICMOS picture emission from excited molecular gas is in blue while stars and hot interstellar dust are yellow-orange.The brightest object in the NICMOS image is a hot massive star enshrouded in dust and completely invisible in the WFPC2 image (R. Thompson, S. Stolovy, C.R. O'Dell, and NASA).

(f) Starburst Galaxies and their Triggering Mechanisms

WFC3 will observe intense "starbursts" in other galaxies (Figure 17.) The triggering mechanisms of such unusual episodes are not understood. Furthermore, the link between starbursts and their host galaxies provides clues to the evolution of galaxies as a whole, and ultimately will clarify the connection between low- and high-redshift galaxies. WFC3's panchromatic design extends observations into the ultraviolet, where the most massive stars formed in a starburst are observable, as well as into the infrared, where the youngest stars still swaddled in dust can be unveiled. The combination of this information allows the mass distribution of the stars formed in the starburst to be inferred, and allows comparison to star formation in less energetic environments such as those found in the Milky Way.

Similarly, the impact of super-winds from active galactic nuclei is poorly understood. Studying the enormous energy released by these winds, as well as physical phenomena which drive them, will yield clues to their role in the evolution of galaxies from high to low redshifts. In particular, with its wide band coverage and selection of special emission-line filters, WFC3 is by far the best tool for such studies.

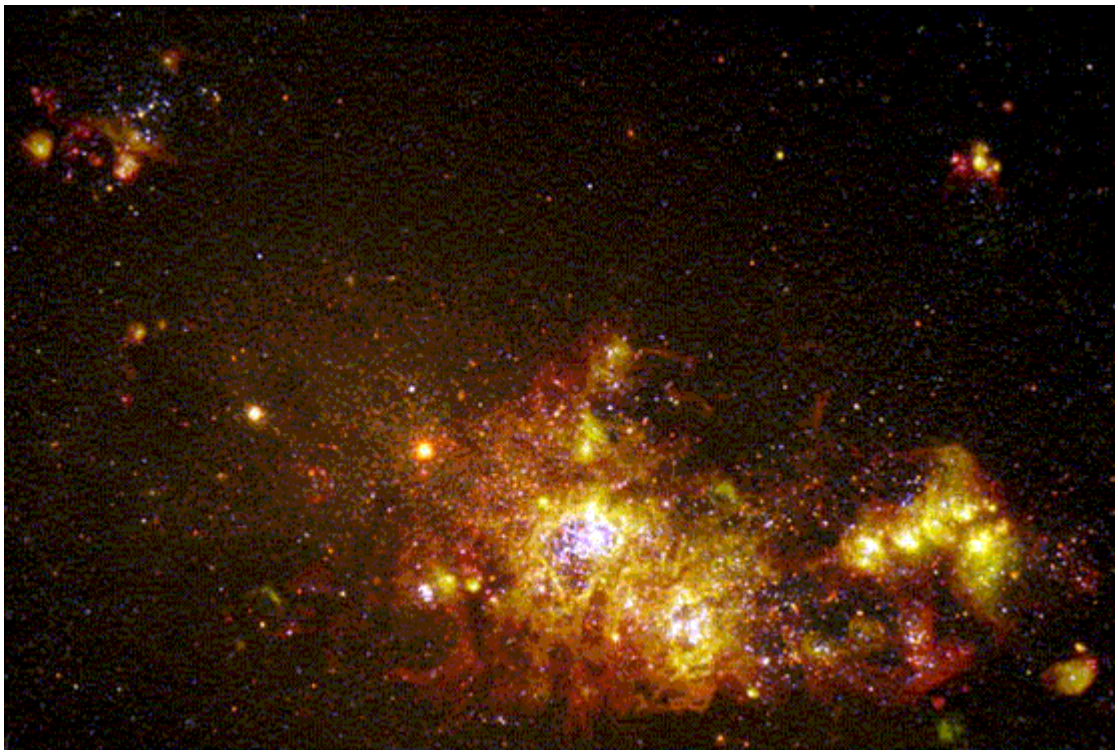

Figure 17. “True” color image of the starburst galaxy NGC 4214 (Hubble Heritage Team, J. W. MacKenty and NASA.) Visible are the older diffuse stellar population (in red), star formation regions (white), and gas filaments (in yellow.)

6.3 Meteorology of the Outer Planets

WFC3 will be a prime instrument for studying weather patterns and climatic variations on the outer planets. Given their very long orbital periods (12 years for Jupiter, 30 for Saturn), the evolution of the weather patterns requires monitoring over long timescales (Figure 18.) Moreover, high sensitivity is required since data have to be collected with high spatial resolution and with integration times short enough to avoid smearing due to the rotation of the planet (for all outer planets the day is less than 24 hours long). Studying the weather on other planets will improve our knowledge of terrestrial weather by allowing meteorologists to refine their models. WFC3 will dramatically improve the already excellent capability of HST in this field. A few examples are illustrated below.

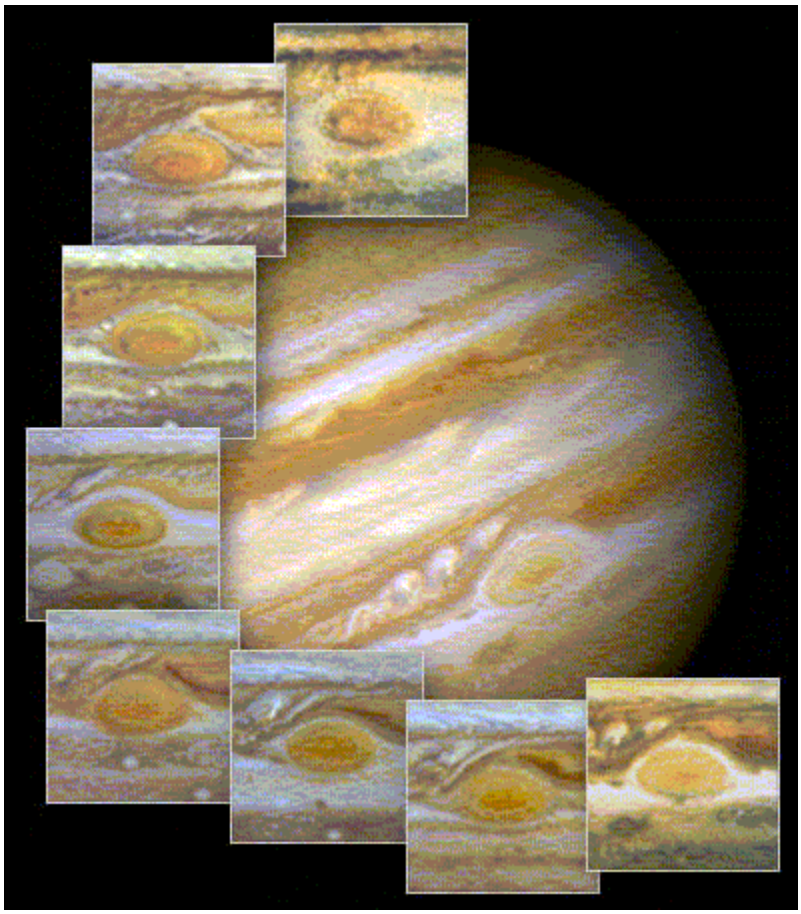

Figure 18. Jupiter's Great Red Spot evolution in the period 1992-1996 as revealed by WFPC2. (Hubble Heritage Team, A. Simon and NASA.) WFC3 will be able to carry out similar studies in the visible and in the near-IR, probing to different depths in the Jovian atmosphere.

Cloud activity in the atmosphere of Uranus is changing rapidly as the planet approaches its equinox (2007). In contrast to the bland and featureless planet seen during the *Voyager* spacecraft encounter in 1986 at the time of solstice, methane band images taken now with WFPC2 on HST show clouds forming and dissipating on timescales of several to tens of days. These short- and long-term changes appear to mark a major alteration in the thermal structure and circulation regimes on a seasonal timescale, now seen for the first time. Images of Uranus with the near-IR channel on WFC3 in a strong methane band (e.g., 1.38 μm), augmented by nearly simultaneous images in the weak (0.62 μm) and medium strength (0.89 μm) methane bands with the UVIS channel, will establish the nature of the changes in greater detail than previously available, since each methane band probes a different depth in the Uranian atmosphere.

The atmosphere of Neptune (see Figure 19) undergoes episodic outbursts, during which time the global brightness in the near-IR changes by nearly a factor of four. Observations in the methane band similar to those outlined for Uranus would be valuable in probing Neptune's atmosphere to understand the source of these outbursts.

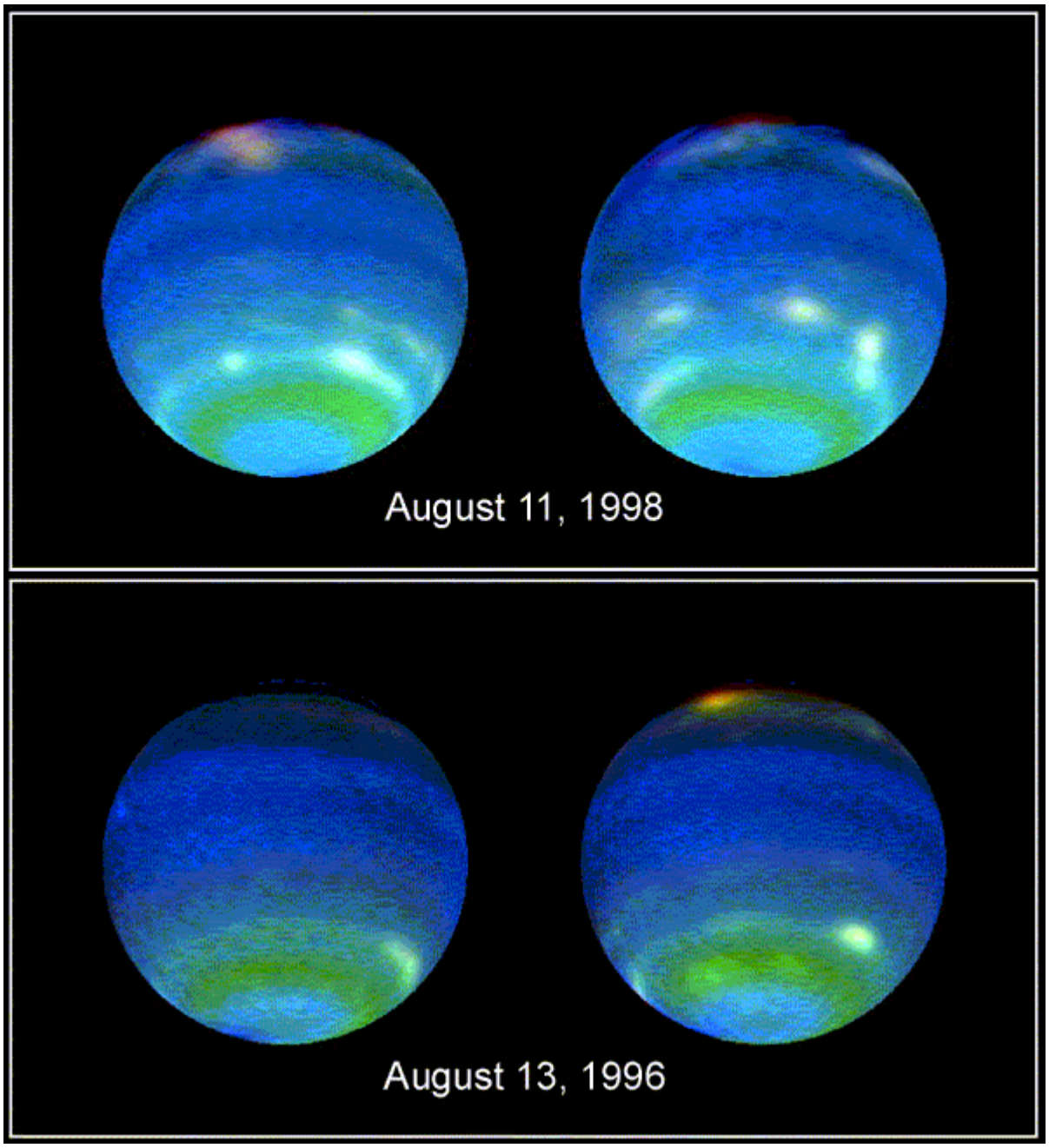

Figure 19. Dynamic weather patterns in Neptune as shown in WFPC2 images (L. Sromovsky and NASA). Each panel shows the short term evolution of cloud patterns on Neptune with 900 miles an hour winds and huge storms the size of the Earth coming and going with regularity.

The atmosphere of Titan is a prime target of the Cassini/Huygens mission currently en route to the Saturn system. The satellite's surface has been observed with HST at near-IR wavelengths where methane opacity is low and particulate scattering is minimal. Two years of more detailed and more sensitive images with WFC3-IR would provide the characteristics of Titan's variable atmospheric activity and some aspects of the surface, establishing the context for the

Cassini/Huygens encounters that will begin in 2004.

7. WFC3 in the Broader Context of NASA and Ground-Based Astronomy

The next decade marks an important transition in astronomy. A number of sensitive, ambitious sky surveys are being undertaken in the UV, optical, and IR bands both in space and on the ground. NASA will be placing a great deal of emphasis on infrared astronomy, for which the premier instrument by 2010 will be NGST. Two of HST's most important roles in the 2004-2010 period will be to exploit the rich return from the new sky surveys and to serve as a bridge to the next generation of powerful instrumentation. In this section we address the contributions of WFC3 in the context of other space- and ground-based initiatives.

7.1 Major UV, Optical, and Infrared Programs

(a) Next Generation Space Telescope

The Next Generation Space Telescope (NGST) will have an 8 meter aperture covering the wavelength range from 1 – 5 μm (with a stretch goal of 0.5 to 30 μm) and a planned lifetime of 5 – 10 years. Its spectral coverage includes the WFC3/IR range. It is currently slated for launch in 2009 to a location at the second Lagrangian point of the Earth-Sun system. The instruments on board will include cameras and spectrometers, but the specific instruments have not yet been selected. Its combination of large collecting area, cool optics, high quantum efficiency, and large field of view (~240 arcsec × 240 arcsec) provides scientific opportunities that extend well beyond the capabilities of HST.

WFC3/IR can serve as a scientific bridge to NGST and it should undertake as much of the basic exploration of the high-resolution, near-infrared universe as possible, leaving NGST free to emphasize those critical projects for which it is essential.

(b) Stratospheric Observatory for Infrared Astronomy

SOFIA is a 2.5-meter infrared telescope which will be flown on a Boeing-747. It is scheduled to begin operation in late 2002. It will have spectral coverage from 0.3 – 1000 μm, but with seeing limitations to ≧2 arcsec in the 0.3-2 μm band. The high spatial resolution of WFC3 will be complementary to SOFIA in the overlapping wavelength range.

(c) Space Infrared Telescope Facility

SIRTF is a 0.85-meter, cooled infrared telescope with a field of view of 1.8 degrees, scheduled for launch in December 2001. It has a planned lifetime of 2.5 - 5 years and will cover the range from 3 - 180 μm. Its cameras have low spatial resolution (about 2 arcsec). Thus, WFC3-IR and SIRTF offer complementary capabilities from the standpoint of both resolution and spectra coverage.

(d) Far Ultraviolet Spectroscopic Explorer

FUSE is an ongoing mission offering high resolution spectroscopy at far-ultraviolet wavelengths between 900 and 1200 Å. Its optimized for brighter, stellar targets. Its capabilities are entirely complementary to WFC3/UVIS.

(e) Space Interferometry Mission

SIM is a mission aimed at obtaining high accuracy astrometric measurements of sources across the sky and at obtaining extremely high angular resolution images. Its emphasis will be on very high angular resolution for relatively bright, visible light sources in selected, small, fields. There is no direct overlap with WFC3 capabilities, although the combination of WFC3 and HST's astrometry Fine Guidance Sensor (FGS) could prove useful as finder probes of important SIM fields.

(f) Galaxy Evolution Explorer

The GALEX mission will make a deep, low spatial resolution (5 arcsec) UV survey of the sky. This will be the first all-sky UV survey since TD-1, which reached only 9th magnitude and did not detect a single galaxy or QSO. GALEX should detect galaxies down to ~21 mag. WFC3 will provide the ideal means for obtaining deeper, higher-resolution follow-up observations of GALEX detections, particularly in the case of interacting galaxies or groups and clusters of galaxies.

(g) Two Micron All Sky Survey

The Two Micron All Sky Survey (2MASS) is a near-infrared (1.2 μm – 2.2 μm) survey of the entire sky. The survey employs highly automated 1.3-meter telescopes at Mount Hopkins Observatory for the northern hemisphere and at Cerro Tololo Inter-American Observatory for the southern hemisphere. It is reaching limiting magnitudes of ~15 in H. The survey should be completed in the course of the year 2000. WFC3-IR is able to image sources more than 10 magnitudes fainter than 2MASS and thus it is ideally suited to carry out follow-up observations of sources that are discovered by 2MASS.

(h) Sloan Digital Sky Survey

The Sloan Digital Sky Survey (SDSS) is a ground-based imaging and spectroscopy program to survey approximately 1/4 of the sky using 5 filters in the range 3500 - 9100 Å. The limiting AB magnitude is 22.6 in the Gunn g filter (4800 Å). Over 100,000,000 astronomical objects, mostly galaxies, will be cataloged. The survey should be completed around the year 2003. WFC3 includes the Sloan filters in its filter complement. Both WFC3 and ACS will be prime instruments for high-resolution imaging follow-up of important discoveries by the SDSS. WFC3 is especially important for extending ACS wide-field coverage into the near-UV and near-IR spectral ranges.

(i) Far Infrared and Sub-millimeter Telescope

The Far InfraRed and sub-millimeter Telescope is an European Space Agency-led mission planned for launch in 2007 and covering the wavelength interval 60-670 μm. FIRST main goals are the study of star formation in dust-enshrouded environments both in the local universe and at high redshift, the physics of the interstellar medium, and solar system investigations. Its science capabilities and goals are complementary to those of WFC3.

(j) Chandra X-ray Observatory

The Chandra X-ray observatory was launched in July 1999. Chandra has a spatial resolution of 0.5 arcsec, and is capable of imaging and spectroscopy in the energy range 0.1-10 keV (1-100 Å.) WFC3 will complement Chandra by allowing the identification of visible/near-infrared counterparts of Chandra sources. In particular, WFC3 will allow the identification of the parent galaxies of dust obscured AGNs, clarify ISM and IGM processes, shed light on the hyper-novae paradigm for Gamma Ray Bursts, allow detailed mass modeling of galaxy clusters.

(k) Adaptive Optics on Ground Based Telescopes

Natural guide-star adaptive optics (AO) systems are now being developed on 8- and 10-meter telescopes. These systems perform best in the near- and mid- IR, but significant corrections can be achieved over the wavelength range spanned by the near-IR channel on WFC3. Presently available AO systems, and those expected in the next several years, have limited fields of view (~30 arcsec) and Strehl ratios well below unity. The wide field, low background, and uniform and stable diffraction limited PSF provided by the WFC3 offer complementary capabilities when compared to AO from the ground. Perhaps the greatest promise of ground-based adaptive optics systems lies in near-IR spectroscopy, where the impact of the background can be minimized by observing between the atmospheric OH lines. WFC3 can play a vital role in identifying appropriate targets for AO-fed spectrographs on US and international 8 to 10 meter telescopes in the years before the launch of NGST.

8. Conclusions

WFC3 is a two-channel camera covering the wavelength interval 2000-17000 Å, a broader interval than that of any previous instrument on the Hubble Space Telescope. Its high sensitivity and large field of view will open up a large new volume in discovery space and allow WFC3 to provide fundamental contributions to a broad array of science problems, including many open problems within NASA's Origins theme. In particular, WFC3 will be able to establish the star formation history of nearby galaxies, to follow the assembly of galaxies during the period of peak star formation and metal production activity 8-12 billion years ago, to explore the birth and death of stars, to study water ice on Mars and the meteorology of the giant planets in the Solar System, and to place constrains on the *End of the Dark Ages* – the high-redshift epoch when the Universe become transparent to ultraviolet photons.

The compelling science made possible by the panchromatic WFC3 will assure that HST will continue to provide forefront science through the end of its mission, and will provide a natural stepping stone from current state-of-the-art capabilities to those of the NGST era.

9. Appendix : WFC3 Design Considerations

9.1 Overview

The design of WFC3 was driven by the need to provide high sensitivity over a broad wavelength region, excellent spatial resolution, and stable and accurate photometric performance. To cover the wavelength interval from 2000 Å to 1.7 μm, the WFC3 provides two science channels: the UVIS channel uses CCD detectors to support imaging between 2000 Å and 10500 Å, while the IR channel uses a HgCdTe detector array to image between 8000 Å and 1.7 μm. Both channels view the same on-axis field in the HST focal plane, but not simultaneously; a channel select mechanism is included to divert the light into the IR channel when this channel is used. An important driver in the design of WFC3 has been cost effectiveness. Hence, WFC3 will reuse hardware that flew on WF/PC as well as reuse designs from NICMOS, STIS, and ACS.

The UVIS channel is optimized for performance in the 2000 Å – 4000 Å wavelength interval, greatly enhancing HST's surveying capabilities at these wavelengths. The UVIS channel consists of an optical train providing focus and alignment adjustment and correction for the HST Optical Telescope Assembly (OTA) spherical aberration, a filter element selection mechanism, a shutter, and a CCD detector assembly. These are supported by a thermal control subsystem and also by control and data handling electronic subsystems. In general concept and functionality, as well as in many design details, this channel is patterned after the ACS/WFC channel.

The IR Channel consists of a selection mechanism to divert light from the UVIS channel, a separate optical train providing focus and alignment adjustment and correction for the spherical aberration, a filter element selection mechanism, and a HgCdTe detector assembly. These are supported by a thermal control subsystem and also by control and data handling electronic subsystems. This channel will be operated in a similar fashion to the NICMOS cameras.

9.2 UVIS Channel

9.2.1 Field of View and Pixel Size

The field of view of WFC3 is limited to 160 x 160 arcsec by the size of the pick-off mirror (POM), which is constrained to avoid vignetting of other science instruments. Cost considerations lead the project to re-use the ACS/WFC camera-head design with 4096 x 4096 pixels in the focal plane. The pixel scale of 0.040 arcsec/pixel exploits the available field of view while providing good sampling of the Point Spread Function (hereafter PSF) in the visible. In order to increase the surface brightness sensitivity, the UVIS channel includes binned read-out modes (see 9.2.4).

9.2.2 CCD Detector

The UVIS channel has a focal plane populated by two 2048 by 4096 pixels CCDs butted together to yield a total of 4096 by 4096 pixels; the gap between the two chips will be about 15-20 pixels (0.6-0.8 arcsec) wide. The camera head is identical to that of the ACS/WFC channel.

The CCD detector sensitivity is optimized for the spectral interval 2000-4000 Å by adopting UV-optimized anti-reflection coatings on the CCDs and by using aluminum mirrors with magnesium fluoride (MgF_2) coatings in the optical train. The aluminum mirrors required to have sensitivity below ~3500 Å reduce the throughput in the red part of the spectrum by (up to) 15 per cent per reflection. To achieve maximum sensitivity, the detector readout noise should be less than 4 electrons per pixel (with a goal of 2 electrons) and the dark current should be less than 10 electrons per pixel per hour. Such low readout noise and dark current permit background-limited observations in visible broad band filters.

Accurate photometric performance requires uniform response within each pixel and excellent charge transfer efficiency (CTE), which must be stable over a relatively long lifetime in the high-radiation environment where HST operates. The non-optimal CTE characteristics at launch and their further degradation on orbit have been an important limitation for highly accurate photometry with WFPC2. Preliminary tests suggest that this may be a problem for ACS as well. Knowledge about the problem and possible solutions have been incorporated into the high level requirements for the WFC3 CCD detectors. These include providing shielding to the CCD (equivalent to 1 cm of molybdenum as for ACS/WFC) and designing the CCDs with a mini-channel. In addition, an ACS-style post-flash capability will be included to reduce the effects of CTE loss in the later years by increasing the background level so as to fill the charge traps that are responsible for CTE loss.

Another important detector parameter is the modulation transfer function (MTF), which defines how photons impinging at a given location on the detector can generate detected signal in neighbouring locations. This phenomenon affects two areas: the uniformity of response within a pixel, which determines the potential photometric accuracy, and the cross-talk between pixels which degrades the PSF sharpness. Limits to the MTF were derived by requiring less than 10 per cent degradation in PSF width and better than 2 per cent photometry in the visible.

9.2.3 Spectral Elements

The UVIS channel makes use of the refurbished WF/PC Selectable Optical Filter Assembly (SOFA) unit which provides up to 48 filters. The UVIS filters provide broad, medium, and narrow bandpasses between 2000 and 10000 Å. The filter complement (Table 3) was recommended by the SOC with broad input from the astronomical community. It includes very broad band filters for the deepest possible imaging, filters which match the most commonly used filters on WFPC2 to provide continuity with previous observations, filters which are optimized to provide maximum sensitivity to various stellar parameters, and narrow band filters which probe a wide range of different physical conditions in the interstellar medium. A UV prism will also be available to support low resolution (R~200) slitless spectroscopy.

9.2.4 Operating Modes

When the whole array is read, each CCD in the UVIS channel is read out through two amplifiers. In addition to this standard read-out mode, sub-array and binned read-out mode are also supported. The sub-array mode allows the user to specify a sub-array of the desired size within a single CCD chip to be read through a single amplifier. Sub-arrays are used to minimize the read-out time and data volume for cases where repeated short exposures are required (e.g. solar system targets). Two binned read-out modes are supported, with 2 x 2 and a 3 x 3 binning. These allow for better surface brightness sensitivity for low background observations (e.g. for narrow band or UV observations) by reducing the relative contribution from read-out noise. Standard dithering patterns are included in the proposal software; these include patterns which allow for both integral and sub-pixel shifts (by moving the telescope.) These patterns help improving (recovering) the sampling of the PSF and minimizing the effects of detector defects.

9.3 IR Channel

9.3.1 Field of View and Pixel Size

The choice of the optimal pixel size for the IR channel resulted from a compromise between field of view and PSF quality. The latter is clearly very important when studying faint sources near bright sources, as for the cases of quasar host galaxies or crowded field photometry. These considerations led the project to consider in detail the properties of the PSF for the IR channel. The modeling is described in detail in the WFC3 Instrument Science Report 1999-01 “WFC3 Near-IR Channel: PSF and Plate Scale Study”. The conclusions of this study are that image reconstruction techniques are able to satisfactorily reconstruct a good quality PSF as long as the pixel size is below 0.15 arcsec. The final choice of 0.13 arcsec/pixel is dictated by optical packaging considerations. This pixel size yields a field of view of 135 by 135 arcsec.

9.3.2 IR Detector Array

The WFC3 IR detector is a 1024 by 1024 array of HgCdTe detectors on a silicon multiplexer. This array is a direct descendant of the NICMOS 256 by 256 and HAWAII 1024 by 1024 arrays in wide use in astronomy. To eliminate the complication and the limited lifetime of a stored cryogen system, the WFC3 IR detector is cooled with a three stage thermoelectric cooler. With this system, the nominal operating temperature is 150 K. The array sensitivity is optimized in the spectral interval 0.8-1.7 μm. The lower wavelength cutoff is determined by the detector material, substrate and – to some extent – coating. In principle, HgCdTe detector arrays could have sensitivity well below 0.8 μm. The upper wavelength cutoff can be varied by changing the composition of the detector material. A longer cutoff wavelength would increase both the dark current at a given temperature and the background due to thermal emission from the telescope and the optical bench. If compatible with technical constraints, the long wavelength cutoff will be pushed beyond 1.7 μm. The detector read noise after multiple non-destructive read should not exceed 15.0 electrons per pixel (with a goal of 10 electrons per pixel). The sum of detector dark current and thermal background contributions should not exceed 0.4 electrons per pixel per second

(with a goal of 0.1 electrons/pixel/sec). These limits on read-out noise and dark current originate from the requirement of being able to carry out zodiacal background limited broad band imaging in the H band (1.6 μm).

To meet the image quality requirements set by the science program, the pixel cross talk should not broaden the PSF by more than 10 per cent and that photometric accuracy be better than 5 per cent.

9.3.3 Internal and OTA thermal background

Since the IR channel is not enclosed in a dewar, infrared thermal emission from the components in the optical bench creates an additional thermal load on the detector as well as generating a background which effectively increases the level of the dark current. This issue has been addressed by partly by cooling the optical bench and partly by designing a cooled, baffled camera head for the IR detector. This reduces the solid angle at the optical bench temperature seen by the detector, decreasing both the thermal load and the effective background. The filter wheel is also cooled to reduce the contribution to the background due to the potentially high off-band emissivity of the filters. Detailed modeling of the emissivity of the various components was carried out to optimize the design and is described in the document "WFC3 IR Channel In-Band Background".

9.3.4 Spectral Elements

The IR channel filter wheel will have 18 available slots to be apportioned into 14 passband filters, two grisms, an open position, and a blank position (see Table 4). The filter complement recommended by the SOC, with broad community input, covers the extended range 0.6 μm to 1.9 μm and includes broad band filters, medium band filters centered on molecular lines and the nearby continuum, and narrow band filters probing interstellar diagnostic lines. The final selection of filters, in particular the choice between Paschen β and Paschen α, will be determined by the detector cutoff wavelength of the flight array. The two grisms will provide WFC3 with the ability to take slitless spectra of sources at a resolving power of about 140 in the wavelength range 1.1 μm to 1.7 μm and of about 200 in the 0.9 μm to 1.1 μm range.

9.3.5 Operating Modes

The IR channel is read in MULTIACCUM mode, i.e. by performing up to 16 unevenly spaced, non-destructive reads during the integration. On orbit experience with NICMOS shows that this is a very effective read-out mode, able to both reduce the effective read-out noise and correct for most cosmic ray hits. Most IR observations are expected to make use of sub-pixel dithering to improve the PSF sampling. Such patterns are included in the proposal software. The IR channel also supports sub-arrays in order to allow for the short integration times required by bright targets (e.g. the HST standard stars and solar system planets).

Table 3: List of the filters in the WFC3 UVIS channel.

Fname	description	lambda (A)	fwhm (A)
F218W	ISM feature	2175	300
F225W		2250	500
F275W		2750	500
F336W	U, Stromgren u	3375	550
F390W	Washington C	3900	1000
F438W	WFPC2 B	4320	695
F555W	WFPC2 V	5410	1605
F606W	WFPC2 Wide V	5956	2340
F814W	WFPC2 Wide I	8353	2555
F475W	SDSS g	4750	1520
F625W	SDSS r	6250	1550
F775W	SDSS i	7760	1470
F850W	SDSS z	8320	>2000
F350LP	visible long pass	3500	>7000
F300X	very broad U	2000	short
F475X	very broad B	3800	2200
F600LP	red long pass	6000	>4000
F390M		3900	200
F410M	Stromgren v	4105	190
F467M	Stromgren b	4675	230
F547M	Stromgren y	5475	710
F621M	11% fil	6212	640
F689M	11% fil	6886	710
F763M	11% fil	7630	780
F845M	11% fil	8454	870
F280N	MgII 2795/2802	2798	42
F343N	(NeV) 3426	3426	228
F373N	(OII) 3726/29	3732	38
F395N	CaII H&K	3950	61
F469N	HeII 4686	4686	32
F487N	H-b 4861	4867	45
F502N	(OIII) 5007	5013	47
F588N	HeI 5876+NaI	5886	60
F631N	(OI) 6300+(SIII)	6306	54
F645N	Continuum	6455	82
F656N	H-a 6563	6563	14
F658N	(NII) 6583	6585	20
F665N	z (Ha +(NII))	6654	113
F673N	(SII) 6717, 31 & z Ha+(NII)	6731	77
F680N	z (Ha +(NII))	6902	288
F953N	(SIII) 9532	9532	64

Fname	description	lambda (A)	fwhm (A)
Quads			
F191N	CIII) 1909	1909	30
F232N	CII) 2326	2326	36
F243N	(NeIV) 2425	2425	36
F378N	z ((OII) 3727)	3780	80
F387N	(NeIII) 3869	3869	26
F422M	continuum	4220	108
F437N	(OIII) 4363	4364	30
F492N	z (H-b)	4924	78
F508N	z ((OIII) 5007)	5081	112
F575N	(NII) 5755	5755	12
F672N	(SII) 6717	6716	14
F674N	(SII) 6731	6731	14
CH4A	25/km-agt	8890	89
CH4A	2.5/km-agt	9060	91
CH4A	0.25/km-agt	9240	92
CH4A	0.025/km-agt	9370	94
CH4B	CH4 6194	6194	62
CH4B	6194 left and right	6340	63
	(dual passband filter)	6038	60
CH4B	CH4 7270	7270	73
CH4B	7270 cont.	7504	75
P200	UV prism	2000	short
F657N	Wide Ha+(NIII)	6573	94

Table 4: List of the filters in the WFC3 IR channel.

Fname	description	lambda (microns)	fwhm (microns)
F160W	Broad H and Red Grism Ref	1.6000	0.40000
F125W	Broad J	1.2500	0.30000
G141	"Red" Low Resolution Grism	NA	0.60000
F187N	Paschen Alpha	1.8781	0.01880
F184N	Paschen Alpha continuum	1.8350	0.01840
F127M	Water/CH_4 continuum	1.2700	0.07000
F139M	Water/CH_4 line	1.3850	0.07000
G102	"Blue" High Resolution Grating	NA	0.25000
F098M	"Blue" Filter, Blue Grism Ref	0.9850	0.17000
F164N	(FeII)	1.6463	0.01646
F167N	(FeII) continuum	1.6677	0.01668
F153M	H_20 and NH_3	1.5300	0.07000
F128N	Paschen Beta	1.2839	0.01284
F130N	Paschen Beta continuum	1.3006	0.01301
	secondary selection		
F126N	(FeII)	1.2588	0.01259
F132N	Paschen Beta (redshifted)	1.3200	0.01320
F065W	Wide V (for UVIS redundancy)	0.6500	0.30000
F095W	Wide "z"	0.9500	0.30000
F140W	Wide Band spanning J-H bour	1.4000	0.40000

10. Appendix: List of WFC3 SOC and Science IPT Members, and IPT Organization Chart

Scientific Oversight Committee

Bruce Balick, University of Washington

Howard E. Bond, Space Telescope Science Institute

Daniela Calzetti, Space Telescope Science Institute

C. Marcella Carollo, Columbia University

Michael J. Disney, University of Wales

Michael A. Dopita, Mt Stromlo and Siding Springs Observatories

Jay A. Frogel, Ohio State University

Donald N. B. Hall, University of Hawaii

Jeff Hester, Arizona State University

Jon A. Holtzman, New Mexico State University

Gerard Luppino, University of Hawaii

Patrick J. McCarthy, Carnegie Observatories

Robert W. O'Connell, University of Virginia (chair)

Francesco Paresce, European Southern Observatory

Abhijit Saha, National Optical Astronomy Observatory

Joseph I. Silk, Oxford University

John T. Trauger, Jet Propulsion Laboratory

Alistair R. Walker, Cerro Tololo Interamerican Observatory

Bradley C. Whitmore, Space Telescope Science Institute

Rogier A. Windhorst, Arizona State University

Erick T. Young, University of Arizona

Science IPT Members

Laura Cawley, STScI

Edward Cheng, GSFC (lead)

Christopher Hanley, STScI

Robert Hill, GSFC

Patricia Knezek, STScI

Carey Lisse, STScI

Olivia Lupie, STScI

John MacKenty, STScI (deputy lead)

Massimo Robberto, STScI

Massimo Stiavelli, STSCI

Integrated Product Team Organization Chart

WFC3 ORGANIZATION CHART

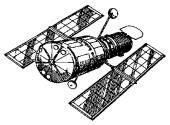

INSTRUMENT MANAGER
Thai Pham

INSTRUMENT SCIENTIST
Ed Cheng

DEPUTY INST. SCIENTIST
John MacKenty

SCIENTIFIC OVERSIGHT COMMITTEE

SYSTEM ENG. IPT
Jim Sneary

GODDARD
Thai Pham
- SYSTEM ENG. Doug Fineberg
- SCIENCE IPT Ed Cheng
- DETECTOR Maliszewski
- IR FILTER R. Boucarut
- STIMULUS Bill Eichhorn
- THERMAL Rick Stavely
- EVA Jill Holz
- ELECTRONICS Ed Cheung
- I & T tbd
- OPTICAL BENCH Jill Holz
- MECHANICAL Sharon Cooper

SWALES
Doug McGuffey
- SYSTEM ENG. Jordan Evans
- OPTICAL BENCH Chris Lashley
- ENCLOSURE Jordan Evans
- RADIATOR Steve Krein
- HEAT PIPES Steve Krein

BALL
Mark Bergeland
- SYSTEM ENG. Bob Slusher
- OPTICS Joe Sullivan
- IR DETECTOR Chris Miller
- UVIS DETECTOR Steve Franka
- ELECTRONICS Mike Malone
- P/L MECHANICAL Raul Martinez
- P/L THERMAL Greg Johnson
- SOFTWARE Chris Dorato
- OPERATIONS T. Schoeneweis

JPL
Linda Herrell
- SYSTEM ENG. Linda Herrell
- SOFA Tom Bickler
- UVIS FILTERS John Trauger
- MECHANICAL Maurice Argoud

NSI
Charlie Diaz
- I&T Dan Hayward

STScI
Chris Blades
- SIPT & OPS John MacKenty

HST CORE TEAM SUPPORT

QA	Rob Sticka
Contracts	Jim Jones
Resources	Kathy Krokos
Schedules	David Turnbo
Safety	Bo Lewis
CM	Kathy Nieman
Contamination	Patsy Dickens
EEE Parts	Rich Williams
Fabrication	Wes Alexander
Metrology	Phil Young
HST S/W	Brian Rehm
SI C&DH	Ron Barasch
HST Systems	Mike Davis
Verification	Kathy Jenkins

1

11. Appendix : Acronym List

ACS – Advanced Camera for Surveys

AO – Adaptive Optics

AGN – Active Galactic Nucleus

CCD – Charge Coupled Device

CTE – Charge Transfer Efficiency

FOV – Field of View

FUSE – Far Ultraviolet Spectroscopic Explorer

HRC – High-Resolution Channel (of the Advanced Camera for Surveys)

HST – Hubble Space Telescope

GALEX – Galaxy Evolution Explorer

HgCdTe – Mercury Cadmium Telluride (near IR detector array)

IDT – Investigation Definition Team

IPT – Integrated Product Team

IR – InfraRed , also channel of the Wide Field Camera 3

keV – one thousand electronvolts

MAMA – Multi-Anode Microchannel Array

MTF – Modulation Transfer Function

MgF2 – Magnesium Fluoride (mirror coating)

NCS – NICMOS Cooling System

NGST – Next Generation Space Telescope

NICMOS – Near-Infrared Camera and Multi-Object Spectrometer

OTA – Optical Telescope Assembly

PC – Planetary Camera (of the Wide Field and Planetary Camera 2)

POM – Pick-Off Mirror

PSF – Point Spread Function

QSO – Quasi Stellar Object

SBC – Solar Blind Channel (of the Advanced Camera for Surveys)

SDSS – Sloan Digital Sky Survey

SIM – Space Interferometry Mission

SIRTF – Space InfraRed Telescope Facility

SOC – Science Oversight Committee

SOFA – Selectable Optical Filter Assembly

SOFIA – Stratospheric Observatory for Infrared Astronomy

STIS – Space Telescope Imaging Spectrometer

STScI – Space Telescope Science Institute

TEC – thermo-electric cooler

UV – UltraViolet

UVIS – Ultraviolet and Visible (channel of the Wide Field Camera 3)

WF – Wide Field (of the Wide Field and Planetary Camera 2)

WFC – Wide Field Camera (of the Advanced Camera for Surveys)

WFC3 – Wide Field Camera 3

WF/PC – Wide Field and Planetary Camera

WFPC2 – Wide Field and Planetary Camera 2

2MASS – Two Micron All Sky Survey

Acknowledgements

The editors want to thank all those who contributed to this document and especially: B. Balick, H. Bond, J. Frogel, J. Hester, J. Holtzmann, P. Knezek, P. McCarthy, M. McGrath, B. Whitmore, E. Young.